

When Calibration Rankings Reverse: Accuracy-Controlled Evaluation for Fair Comparison of LLMs

Zhichao Yang^{1*}, Caiqi Zhang^{2*}, Ruihan Yang^{1*}, Chengzu Li²,
Nigel Collier², Deqing Yang¹

¹Fudan University ²University of Cambridge
{zcyang25, rhyang21}@m.fudan.edu.cn, {cz391}@cam.ac.uk

Abstract

Calibration evaluates whether a model’s confidence aligns with its empirical accuracy. Existing studies often compare the calibration of different large language models using global calibration metrics such as Expected Calibration Error and Brier Score. We begin by showing, both theoretically and empirically, that such comparisons are confounded by differences in model accuracy. For fairer cross-model comparison, we then propose ACE, an accuracy-controlled evaluation framework with three complementary views: Instance-Aligned, Distribution-Aligned, and Candidate-Aligned calibration. Across multiple benchmarks, model families, and confidence elicitation methods, we use ACE to study two practically important comparison axes, small versus large models and thinking versus non-thinking models. We find that many previously reported calibration advantages under raw global metrics weaken substantially after accuracy control. We also find that ranking reversal is frequent: models favored by raw metrics often cease to be favored once accuracy is controlled. Our results show that raw global calibration metrics are not robust for cross-model comparison, and that fair calibration comparison requires accuracy-aware evaluation.

1 Introduction

Large Language Models (LLMs) have achieved remarkable capabilities, making their reliable deployment in high-stakes domains a critical priority (Huang et al., 2024; Wang et al., 2023). In such settings, it is not enough for a model to achieve high average accuracy; it must also indicate how likely its prediction is to be correct. This has made calibration, the alignment between a model’s confidence and its empirical correctness, a central topic in recent work on trustworthy language models (Xiong et al., 2024; Geng et al., 2024). Global

metrics such as Expected Calibration Error (ECE) and Brier Score (BS) are now widely used to quantify the calibration level of an LLM.

A common but underexamined assumption behind this practice is that *global calibration scores are directly comparable across models*. Under this view, if one model achieves lower ECE/BS than another, it is natural to conclude that the former is better calibrated (Zeng et al., 2025; Mei et al., 2025; Yoon et al., 2025; Lacombe et al., 2025). However, we argue that this interpretation becomes problematic when the models being compared differ substantially in task accuracy. A model with higher accuracy can achieve a better global calibration score for two different reasons: it may be truly better calibrated, or it may simply make fewer mistakes. For example, if two models both assign confidence 1.0 to every answer, the more accurate one will automatically score better on ECE/BS, despite identical confidence behavior. In Section 3, we first show that global calibration metrics are confounded by model accuracy, and therefore do not reflect calibration quality alone. This raises a basic but important question: **when two models operate at different accuracy levels, are their calibration scores really being compared on equal footing?**

In this work, we argue that naïve cross-model comparisons based on raw global calibration metrics can be misleading. When models differ greatly in accuracy, raw global metrics can systematically favor the stronger model even when the underlying confidence behavior is not correspondingly better. More importantly, this confound can produce what we term *ranking reversal*: a model that appears better calibrated under raw global metrics can become *less* calibrated once accuracy is controlled. We argue that ranking reversal is a particularly revealing diagnostic for calibration evaluation, because it makes the failure of naïve cross-model comparison directly observable. Rather than merely shifting

*Equal contribution.

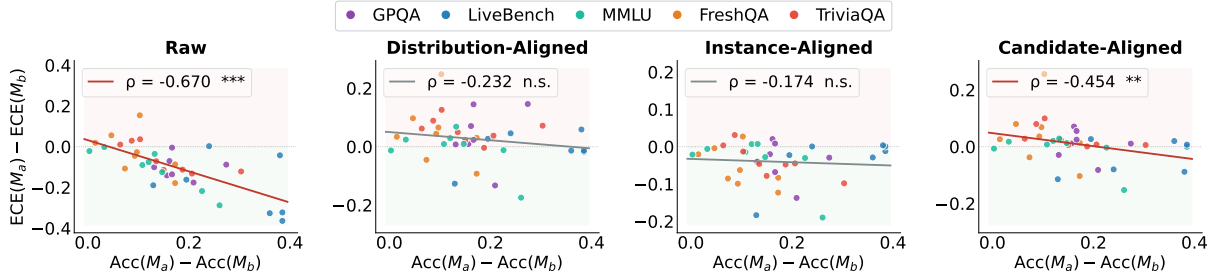


Figure 1: **Accuracy differences strongly confound raw ECE comparison.** Each point is one dataset-level average for a model pair ($\rho = -0.670$, $n = 40$, 95% CI $[-0.81, -0.45]$, $p < 10^{-5}$; Appendix A.2). Larger accuracy gaps correspond to larger raw calibration gaps; our accuracy-controlled views substantially reduce this confound.

the magnitude of a calibration gap, controlling for accuracy can overturn the conclusion about which model is better calibrated.

We therefore propose **ACE** (Accuracy-Controlled Evaluation), a framework for fairer cross-model calibration analysis. ACE compares models under matched or partially matched correctness conditions before drawing calibration conclusions. It includes three complementary views. First, *Instance-Aligned* (IA) calibration compares models only on examples where they share the same outcome, providing strict instance-level control. Second, *Distribution-Aligned* (DA) calibration matches the aggregate outcome composition of the compared models, enabling a broader distribution-level comparison. Third, *Candidate-Aligned* (CA) calibration extends the same principle to evaluative settings with a shared answer space, where models judge a common pool of candidate answers. Together, these three views disentangle calibration quality from task accuracy, which raw global metrics conflate.

Using ACE across multiple benchmarks, model families, calibration metrics, and confidence elicitation methods, we find that many raw calibration conclusions are substantially less stable than they appear. Apparent calibration advantages often shrink once accuracy is controlled, and ranking reversal occurs frequently in both scale-based and thinking-versus-non-thinking model comparisons. These findings do not imply that calibration metrics such as ECE or BS are uninformative. Rather, they show that *raw* global calibration scores are not always apples-to-apples across models with different accuracies. When the goal is fair cross-model comparison, accuracy control is not a minor refinement; it can change the conclusion itself.

- We show that raw comparisons of calibration across models can be misleading when models

differ in accuracy, and identify a key **ranking reversal** phenomenon.

- We propose **ACE**, an accuracy-controlled evaluation framework with three complementary views for fairer comparison.
- Across multiple datasets, model families, and confidence elicitation methods, we show that many apparent calibration advantages weaken substantially under ACE, and that ranking reversals are common enough to materially change model-level conclusions.

2 Related Work

Calibration Metrics and Calibration Methods.

Existing work studies calibration using both visualization-based and scalar metrics. Common examples include the *reliability diagram* and *Expected Calibration Error* (ECE), which summarize the gap between confidence and empirical accuracy across bins (Niculescu-Mizil and Caruana, 2005; Naeini et al., 2015), as well as probabilistic scoring rules such as the *Brier Score* and *negative log-likelihood* (NLL) (Brier, 1950; Lakshminarayanan et al., 2017). Prior work has also examined the sensitivity of ECE-style analysis to evaluation design, including equal-mass, adaptive, and class-conditional variants (Nguyen and O’Connor, 2015; Nixon et al., 2019). To improve calibration, widely used post-hoc methods include *temperature scaling*, *Platt scaling*, and *isotonic regression* (Platt et al., 1999; Zadrozny and Elkan, 2002; Guo et al., 2017), while training-time approaches such as *label smoothing* and *deep ensembles* have also been explored (Pereyra et al., 2017; Lakshminarayanan et al., 2017). These methods are complementary to our work: rather than proposing a new way to recalibrate model confidences, we study whether calibration comparisons themselves are fair when models differ in task accuracy.

Fairness in Calibration Comparison. Recent work has shown that calibration evaluation itself can be sensitive to how it is defined and aggregated (Nixon et al., 2019; Vaicenavicius et al., 2019). In particular, prior studies have shown that calibration conclusions may change with the choice of metric, binning scheme, and aggregation rule, and that standard ECE-style evaluation may reward confidence assignments that reduce aggregate error without improving the separation between correct and incorrect predictions (Si et al., 2022). Other work further suggests that calibration scores should not be interpreted independently of model accuracy, since more accurate models can obtain systematically more favorable scores under standard global metrics (Minderer et al., 2021; Chidambaram and Ge, 2024). Recent proposals such as *CKCE* highlight that relative calibration comparison can be distorted by differences in predictive marginals (Moskvichev and Sejdinovic, 2025). However, these studies overlook a critical question: when models differ in accuracy, how can we fairly compare their calibration to ensure results reflect genuine confidence quality rather than mere task success? Our work addresses this gap by making accuracy the explicit control variable in cross-model calibration comparison and by showing that such control can change not only calibration gaps but also model rankings.

3 Background and Motivation

Reliable confidence estimation is central to the safe deployment of LLMs. A standard lens for studying this property is *calibration*, which asks whether confidence estimates match empirical correctness probabilities. In practice, calibration is often summarized by global metrics such as Expected Calibration Error (ECE) and Brier Score (BS). However, when models differ substantially in task accuracy, such comparisons become problematic. This section introduces the notation and shows, analytically and empirically, why accuracy confounds cross-model calibration comparisons, motivating our accuracy-controlled evaluation framework.

Notation and Standard Metrics. Let $D = \{(x_i, y_i)\}_{i=1}^N$ be an evaluation set, where x_i is an input and y_i is its gold label. Given a model M , let \hat{y}_i denote its prediction and $c_i \in [0, 1]$ the confidence assigned to that prediction. We define the correctness indicator $z_i = \mathbf{1}[\hat{y}_i = y_i]$, and the empirical

accuracy

$$\text{Acc}(M) = \frac{1}{N} \sum_{i=1}^N z_i.$$

To measure calibration, we consider two standard global metrics. First, ECE partitions the confidence range into bins $\{I_b\}_{b=1}^B$ and computes

$$\text{ECE}(M) = \sum_{b=1}^B \frac{|S_b|}{N} |\text{acc}(S_b) - \text{conf}(S_b)|,$$

where $S_b = \{i : c_i \in I_b\}$, $\text{acc}(S_b) = \frac{1}{|S_b|} \sum_{i \in S_b} z_i$, and $\text{conf}(S_b) = \frac{1}{|S_b|} \sum_{i \in S_b} c_i$. Second, the Brier Score is

$$\text{BS}(M) = \frac{1}{N} \sum_{i=1}^N (c_i - z_i)^2.$$

Both metrics are meaningful summaries of confidence quality for a fixed model on a fixed prediction set. Our concern is different: *directly comparing these global scores across models with different accuracies can be severely confounded.*

Why Accuracy Is a Confounder. The core problem is that global calibration metrics depend not only on how confidence is distributed, but also on the proportion of correct versus incorrect predictions. When a stronger model answers more questions correctly, its global ECE or BS can improve mechanically, even if its confidence behavior is not intrinsically better.

Intuitively, global metrics average over correct and incorrect predictions, so changing their mixture can change the score even when confidence behavior is fixed. This can be seen in a simple toy (with more rigorous discussion in Appendix A.1) setting where all predictions receive the same confidence $q \in [0, 1]$. Let $a = \text{Acc}(M)$. Then

$$\begin{aligned} \text{ECE}(M) &= |a - q|, \\ \text{BS}(M) &= a(1 - q)^2 + (1 - a)q^2 \\ &= q^2 + a(1 - 2q). \end{aligned}$$

Thus, BS depends linearly on accuracy. In the practically relevant high-confidence regime $q > 0.5$, $\text{BS}(M)$ decreases as a increases. Likewise, ECE is piecewise linear in a ; under the common overconfident regime $a \leq q$, it simplifies to

$$\text{ECE}(M) = q - a,$$

which also decreases as accuracy increases. Therefore, even when two models exhibit the same nominal confidence level, the more accurate one can obtain a better global calibration score simply because it has more correct predictions.

Empirical Evidence and Motivation. This controlled example motivates an empirical diagnostic. As shown in the “Raw” panel of Figure 1, experiments across mainstream LLM families and benchmark tasks reveal a strong negative correlation ($\rho = -0.670$) between global calibration scores and task accuracy. Models with higher accuracy mechanically appear better calibrated under raw ECE, even when they remain highly overconfident. This pattern validates our concern: a substantial part of the reported “calibration advantage” of stronger models may simply reflect outcome composition rather than genuinely superior uncertainty estimation. This empirical trend motivates the central question of our paper: *how should we compare calibration fairly when models have different cognitive capabilities?*

4 ACE: Accuracy-Controlled Evaluation

We introduce ACE (Accuracy-Controlled Evaluation), a framework for fairer cross-model calibration comparison. The key idea is simple: when two models differ in task accuracy, their raw global calibration scores are not directly comparable because they are computed over prediction sets with different outcome compositions. ACE addresses this by constructing comparison protocols in which predictive success is explicitly controlled before calibration is measured. These views are intended to be read jointly rather than as interchangeable metrics: agreement indicates a stable conclusion, while disagreement identifies the relevant alignment choice. The framework contains two views for *generative calibration*, where models score their own answers, and one complementary view for *evaluative calibration*, where they judge a shared answer space.

Setup. Consider two models, M_A and M_B , evaluated on the same dataset $D = \{(x_i, y_i)\}_{i=1}^N$. For each example x_i , model M_m produces a prediction $\hat{y}_i^{(m)}$, a confidence score $c_i^{(m)} \in [0, 1]$, and a correctness indicator

$$z_i^{(m)} = \mathbf{1}[\hat{y}_i^{(m)} = y_i], \quad m \in \{A, B\}.$$

Let $\text{Acc}(M_m) = \frac{1}{N} \sum_{i=1}^N z_i^{(m)}$ denote the model’s accuracy. A naive evaluation would directly compare global scores like $\text{ECE}(M_A)$ and $\text{ECE}(M_B)$ over the full dataset D . However, as established in Section 3, such comparisons are inherently confounded when $\text{Acc}(M_A) \neq \text{Acc}(M_B)$. To address this, ACE evaluates cross-model calibration strictly under controlled accuracy conditions.

4.1 Instance-Aligned (IA) Calibration

Our first view enforces *instance-level alignment*. We compare two models only on examples where they have the same outcome, *i.e.*, both are correct or both are wrong. Formally, we define

$$D_{\text{both-right}} = \left\{ i : z_i^{(A)} = 1 \wedge z_i^{(B)} = 1 \right\},$$

$$D_{\text{both-wrong}} = \left\{ i : z_i^{(A)} = 0 \wedge z_i^{(B)} = 0 \right\},$$

and $D_{\text{IA}} = D_{\text{both-right}} \cup D_{\text{both-wrong}}$. By construction, the two models have identical empirical accuracy on D_{IA} :

$$\text{Acc}_{D_{\text{IA}}}(M_A) = \text{Acc}_{D_{\text{IA}}}(M_B) = \frac{|D_{\text{both-right}}|}{|D_{\text{IA}}|}.$$

This makes D_{IA} a particularly clean comparison set: because correctness is aligned **instance by instance**, calibration differences can be interpreted more directly as differences in confidence assignment rather than differences in task success. IA retains substantial coverage in our experiments ((median 78.0%, IQR [66.3%, 82.2%], min 55.2%; Appendix E.4).).

We then compute calibration metrics (*e.g.*, ECE and BS) on D_{IA} . A useful feature of IA is its decomposition. $D_{\text{both-right}}$ captures shared competence, while $D_{\text{both-wrong}}$ captures shared blind spots. The latter is especially informative: if a stronger model still assigns systematically higher confidence on $D_{\text{both-wrong}}$, then its apparent global calibration advantage may partly mask a more severe form of overconfidence on questions that neither model actually understands. This instance-aligned analysis therefore reveals *where* calibration differences come from, not merely whether one global score is lower than another.

4.2 Distribution-Aligned (DA) Calibration

Our second view enforces *distribution-level alignment*. Instead of matching models instance by instance, DA matches the overall outcome composition so that calibration is compared under a common effective accuracy level. Concretely, rather

than requiring the two models to agree on the same instances, DA only requires them to be compared under the same aggregate proportion of correct and incorrect predictions.

A natural way to achieve this is to rebalance one model’s predictions to match the empirical accuracy of the other. One implementation is resampling, which selectively discards observations until the target outcome composition is reached. While simple, this approach introduces sampling variance and reduces effective sample size. We therefore consider a more rigorous alternative that retains all observations: *Distribution-Aligned* (DA). Widely used in causal inference to correct for confounded comparisons (Rosenbaum and Rubin, 1983), DA reweights each prediction so that the weighted outcome composition matches a target accuracy (see Appendix B for a detailed justification).

Let $a_A = \text{Acc}(M_A)$, $a_B = \text{Acc}(M_B)$ with $a_A > a_B$. To evaluate M_A at the accuracy level of M_B , we define

$$w_i^{(A)} = \begin{cases} a_B/a_A & \text{if } z_i^{(A)} = 1 \\ (1 - a_B)/(1 - a_A) & \text{if } z_i^{(A)} = 0 \end{cases},$$

which satisfies $\sum_i w_i^{(A)} z_i^{(A)} / \sum_i w_i^{(A)} = a_B$. Thus, the weighted correctness composition of M_A matches the target accuracy a_B . The resulting DA calibration metrics are computed as:

$$\text{DA-BS}_{a_A \rightarrow B} = \frac{1}{W} \sum_i w_i^{(A)} \left(c_i^{(A)} - z_i^{(A)} \right)^2,$$

$$\text{DA-ECE}_{a_A \rightarrow B} = \sum_{b=1}^B \frac{W_b}{W} |\text{acc}_w(S_b) - \text{conf}_w(S_b)|,$$

where $W = \sum_i w_i^{(A)}$ is the total weight, $W_b = \sum_{i \in S_b} w_i^{(A)}$ is the bin weight, and acc_w and conf_w are weighted bin-level accuracy and confidence.

DA trades the strictness of IA for broader coverage. Rather than enforcing agreement on the same individual instances, it aligns only the overall distribution of correct and incorrect outcomes, allowing comparison on a larger effective sample. This makes DA a useful test of whether an apparent calibration advantage persists once differences in aggregate outcome composition are removed.

4.3 Candidate-Aligned (CA) Calibration

The two views above concern *generative calibration*: each model generates its own answer and reports confidence on that answer. Our third view

removes this asymmetry by aligning the *candidate answer space*.

For each input x_i , let $s_i^{(A)}$ and $s_i^{(B)}$ be the answers generated by M_A and M_B , and define the shared candidate pool $U_i = \{s_i^{(A)}, s_i^{(B)}\}$. More generally, U_i can include any set of candidate answers under consideration. Each model then evaluates every candidate in the same pool. Let $e_i^{(m)}(s) \in [0, 1]$ denote model M_m ’s confidence that candidate $s \in U_i$ is correct, and let $y_i(s) \in \{0, 1\}$ be the ground-truth correctness label of candidate s . CA is then computed at the *candidate level*: each pair (x_i, s) is treated as one evaluation instance, and calibration compares $e_i^{(m)}(s)$ against $y_i(s)$ over all i and all $s \in U_i$. For example,

$$\text{CA-BS}(M_m) = \frac{1}{\sum_i |U_i|} \sum_i \sum_{s \in U_i} \left(e_i^{(m)}(s) - y_i(s) \right)^2$$

with CA-ECE defined analogously by binning the values $e_i^{(m)}(s)$ across all candidate-level instances.

As both models score the same candidates, CA controls for differences in generation space and isolates calibration in evaluation mode. It also exposes *self-preference bias*: a model may assign higher confidence to its own answer than to a competing answer, even when the competing answer is better supported.

5 Experiments

5.1 Experiment Setup

Models. We study models along two comparison axes: *small vs. large* and *thinking vs. non-thinking*. For scale-based comparison, we evaluate Qwen2.5 (7B and 72B) (Qwen et al., 2025), LLaMA 3.1 (8B and 70B) (Grattafiori et al., 2024), and GPT-OSS (20B and 120B) (OpenAI et al., 2025). For reasoning-mode comparison, we evaluate Qwen3 (8B and 32B) (Yang et al., 2025) and GPT-OSS (20B and 120B) under different reasoning settings (OpenAI et al., 2025). These comparison axes are motivated by prior findings that larger models often produce better calibrated confidence estimates than smaller ones, although the gains can be task-dependent (Xiong et al., 2024; Fang et al., 2025). Prior work also suggests that reasoning-enabled models often calibrate better than non-reasoning models on reasoning-intensive tasks, while the picture is more mixed on factual knowledge tasks (Yoon et al., 2025; Zeng et al., 2025). Additional inference settings and answer-generation prompts are provided in Appendix C and Appendix D.1.

Datasets. We evaluate on five datasets spanning two categories: *knowledge-based* and *reasoning-based* tasks. The knowledge-based datasets are FreshQA and TriviaQA (Vu et al., 2023; Joshi et al., 2017), both in an open-ended factual QA format. The reasoning-based datasets are GPQA Diamond, LiveBench, and MMLU-Pro (Rein et al., 2023; White et al., 2025; Wang et al., 2024), which cover expert-level multiple-choice reasoning, general reasoning, and academic problem solving, respectively. The answer formats include both open-ended and multiple-choice settings. Additional dataset details are provided in Appendix D.2.

Confidence Elicitation Methods. We consider three representative confidence elicitation methods: *verbalized confidence* (Tian et al., 2023), $P(\text{True})$ (Kadavath et al., 2022), and *self-consistency* (Wang et al., 2022; Manakul et al., 2023). Additional prompting templates and implementation details are provided in Appendix D.3.

5.2 Main Results

Ranking reversal occurs frequently, and this pattern is robust across metrics and confidence elicitation methods. We define a *ranking reversal* as a case where the model that appears better calibrated under the raw comparison becomes less calibrated after ACE. In Figures 2 and 3, such reversals correspond to points falling in the first and third quadrants, where the raw and ACE-based comparisons disagree in sign. We widely observe ranking reversals under both ECE and BS, and across confidence estimates. This means that calibration conclusions drawn from raw global metrics can be misleading when the compared models differ in accuracy.

For scale-based comparisons, the calibration advantage of larger models weakens markedly after ACE. Figure 2 shows that, when comparing Qwen2.5, LLaMA 3.1, and GPT-OSS model pairs, reversal rates are common across all three confidence elicitation methods and both metrics. Depending on the setting, the reversal rate ranges from 13% to 60%, with the strongest effects typically appearing under Distribution-Alignment and Instance-Alignment. For example, under verbalized confidence, the reversal rate reaches 60% for one metric under DA, and under $P(\text{true})$ it reaches 50% in some settings. These results indicate that part of the apparent calibration advantage of larger models under raw global metrics is attributable to

their higher task accuracy rather than to uniformly better confidence quality.

For thinking-versus-non-thinking comparisons, controlled evaluation also overturns many raw rankings. Figure 3 shows the same qualitative pattern when comparing thinking and non-thinking modes within the same model family. Here, reversal remains frequent after accuracy alignment, and in some settings becomes even more pronounced: for instance, under self-consistency, the reversal rate reaches 65% when Candidate-Aligned, while several Distribution-Aligned settings fall in the 30%–53% range. Even under verbalized confidence, where CA can be relatively conservative, DA and IA still produce substantial reversal rates such as 33% and 53%. This suggests that some of the raw calibration gains attributed to thinking are mediated by improved answer accuracy, rather than reflecting a purely metacognitive improvement in confidence estimation.

Taken together, the results show that raw global calibration scores are often not apples-to-apples across models with different accuracies. Our main empirical finding is therefore not that larger or thinking models are poorly calibrated, but that raw global calibration metrics can confound confidence quality with outcome composition. Once accuracy is explicitly controlled, several widely reported calibration advantages shrink substantially, and in many cases the ranking itself changes. These findings support the use of ACE-style evaluation as a standard companion to raw calibration reporting when the goal is fair cross-model comparison.

6 Analysis

Distribution-Aligned (DA) and Instance-Aligned (IA) usually overturn raw winners together, while Candidate-Aligned (CA) more often acts alone. As shown in Figure 4, the dominant reversal structure is not arbitrary: across all 120 cases, the three most common patterns are no reversal (28.3%), CA-only reversal (20.8%), and joint DA+IA reversal (20.0%), which together account for 69.2% of all comparisons. More importantly, DA and IA share the same reversal status in 79.2% of cases, whereas CA more often departs from them as a separate comparison axis. This suggests that DA and IA often capture related corrections to the raw ranking, even though the structure is not fully binary, since all-three reversal

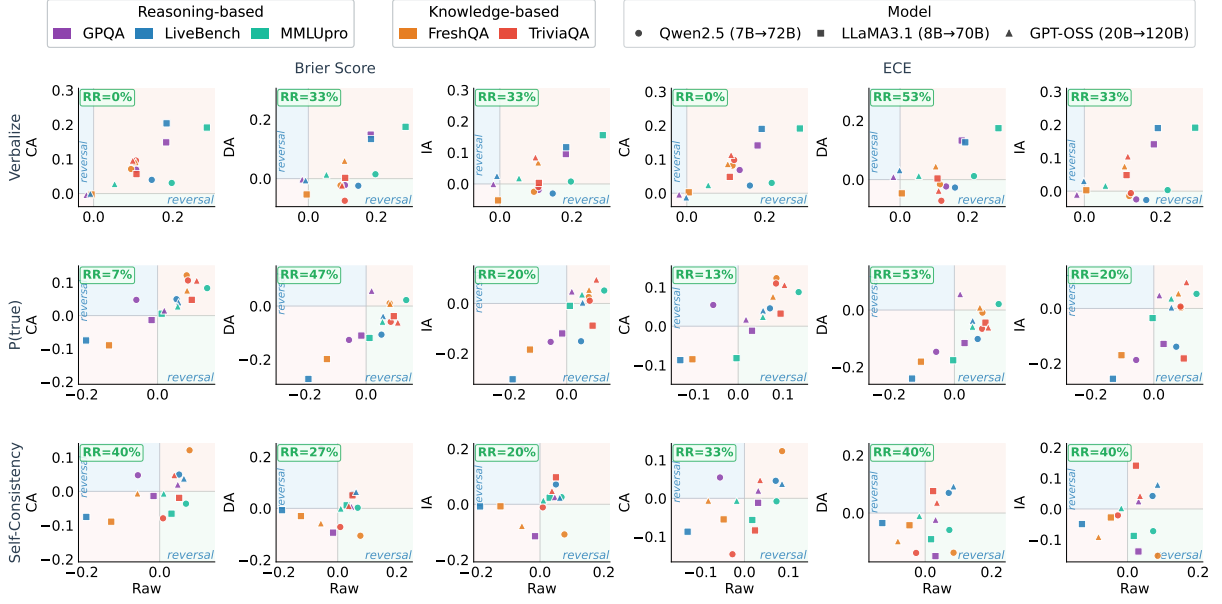


Figure 2: Calibration gap between small and large models within the same family, plotted before (x -axis, *Raw*) and after accuracy alignment (y -axis). Each point represents one (dataset, calibration metric, confidence elicitation method) combination. Points in **Quadrants II and IV** (*reversal*) indicate cases where the raw and alignment-based rankings disagree: the model favored by raw ECE/BS is no longer favored after accuracy control.

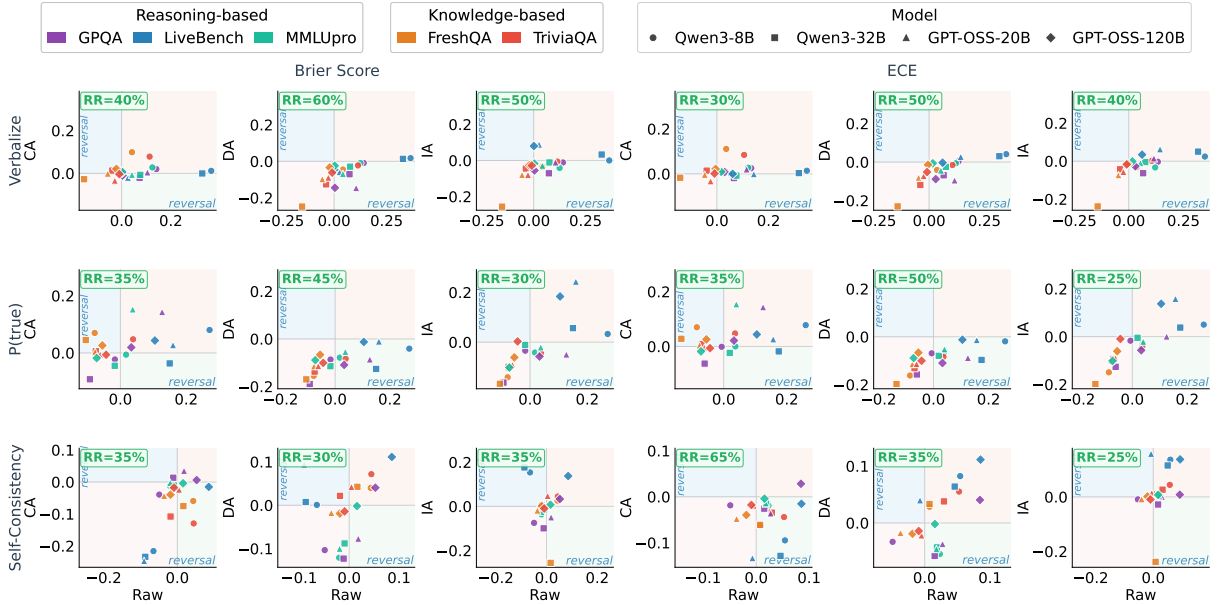


Figure 3: Calibration gap between non-thinking and thinking models, using the same setup as Figure 2.

still occurs in 10.0% of cases. The same asymmetry also appears in the knowledge-versus-reasoning split: across method-level reversal rates, DA and IA generally move in more similar directions, whereas CA is more likely to diverge. This asymmetry is also consistent with the definitions of the three views. DA and IA both still evaluate confidence on each model’s own answers and mainly differ in how they align accuracy, whereas CA changes the candidate answer pool itself and

therefore more easily yields a separate ranking.

The source of reversal depends strongly on the confidence method. Table 1 shows that the three confidence methods do not share a single reversal signature. Verbalized confidence is dominated by joint DA+IA reversal (35.0%), suggesting that its raw ranking is especially sensitive to distribution-aligned and instance-aligned comparison. SC follows a different pattern: CA-only reversal is the

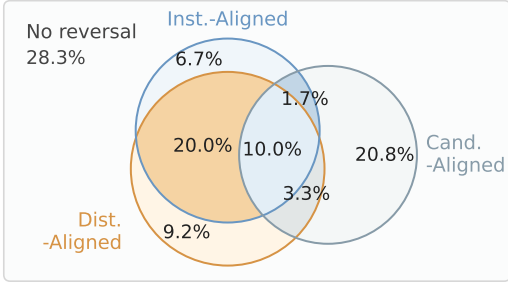


Figure 4: Overall reversal-combination distribution relative to the raw ECE winner. The figure highlights that Dist.-Aligned and Inst.-Aligned agree in 79.2% of cases, whereas Cand.-Aligned more often behaves as a separate comparison axis.

Method	Exclusive RR (%)			NRR (%)
	IA	DA	CA	
Verbalized	7.5	2.5	7.5	27.5
P(True)	2.5	22.5	20.0	30.0
SC	10.0	2.5	35.0	27.5

Table 1: Method-level ranking reversal rates (RR). IA, DA, and CA columns report the fraction of cases where *exclusively* that view overturns the Raw ECE winner. NRR (no-reversal rate) is the fraction of cases where no view overturns the Raw ECE winner.

most common outcome (35.0%), indicating substantially greater sensitivity to candidate-pool alignment than to DA or IA comparison. P(True), in contrast, shows the most diffuse profile, with substantial mass on both DA-only (22.5%) and CA-only (20.0%) reversals rather than a single dominant pattern. The key point is not merely that reversal frequencies differ, but that different methods are destabilized by different kinds of alignment.

Dataset structure determines which kind of reversal becomes dominant. As illustrated in Table 2, reversal consistency is also highly dataset-dependent. MMLU-Pro exhibits the highest no-reversal rate (50.0%), indicating comparatively stable raw rankings. By contrast, FreshQA and TriviaQA are more often dominated by CA reversals (45.8% and 33.3%, respectively), suggesting that candidate-pool alignment plays a larger role in open-ended knowledge QA. GPQA Diamond has the highest all-three-reversal rate (16.7%), meaning that its raw winner is more likely to be overturned jointly by all three aligned views. LiveBench Reasoning shows the most diffuse pattern, with mass spread across several reversal types rather than concentrated in a single dominant signature. Taken

Dataset	Exclusive RR (%)			NRR (%)
	IA	DA	CA	
FreshQA	8.3	4.2	45.8	25.0
GPQA	0.0	16.7	12.5	25.0
LiveBench	16.7	12.5	8.3	20.8
TriviaQA	8.3	8.3	33.3	20.8
MMLU	0.0	4.2	4.2	50.0

Table 2: Dataset-level ranking reversal rates (RR). IA, DA, and CA columns report the fraction of cases where *exclusively* that view overturns the Raw ECE winner.

together, these dataset-level differences indicate that the stability of raw ECE ranking depends not only on the confidence method, but also on task format and evaluation structure.

Additional analyses on reversal patterns and confidence distributions are in Appendix E.

Practical Recommendations. We recommend using DA as the default reporting metric, as it retains the full sample and agrees with IA in 79.2% of cases (Figure 4). IA should serve as a corroborating check; their agreement indicates a stable conclusion. Finally, treat CA as a diagnostic tool: if CA diverges from DA and IA, the ranking is likely sensitive to candidate-pool alignment rather than indicating a robust reversal.

7 Conclusion

We introduced ACE, an accuracy-controlled evaluation framework for fairer calibration comparison in large language models. Our analysis shows that standard global calibration metrics can be substantially confounded by differences in task accuracy, making raw cross-model comparisons misleading. To address this, ACE provides three complementary views that compare models under matched or partially matched correctness conditions. Across model families, datasets, and confidence elicitation methods, we find that many apparent calibration advantages weaken once accuracy is controlled, and that ranking reversals are common, suggesting that standard evaluation can overstate the metacognitive advantage of stronger models. Our results highlight the importance of accuracy-aware calibration analysis and position ACE as a useful companion to conventional calibration reporting for more reliable assessment of LLM confidence quality.

Limitation

Our study also has several limitations that suggest directions for future work. First, our experiments focus on open-source models, which allow controlled and reproducible evaluation across model families, but further validation on proprietary systems would be valuable to assess how broadly the observed trends extend. Second, while ACE provides three complementary views for accuracy-controlled comparison, each view has its own trade-off: IA offers strict instance-level control but depends on shared-outcome coverage, DA retains the full sample through reweighting but relies on distributional alignment, and CA exposes candidate-pool and self-preference effects but should be read as diagnostic rather than as a replacement for own-output calibration. Accordingly, we interpret the three views jointly rather than treating any single view as a complete solution. Finally, the current formulation of ACE is based on a binary correctness variable, $z_i \in \{0, 1\}$, which is a natural fit for multiple-choice and exact-match benchmarks but less directly applicable to open-ended generative tasks, where performance may be graded with partial credit or other continuous measures. Extending the framework to such settings is an important direction for future research.

Ethics Statement

Our research adheres to strict ethical guidelines. We verified the licenses of all software and datasets used in this study to ensure full compliance with their terms. No privacy concerns have been identified. We have conducted a thorough assessment of the project and do not anticipate any further risks. We only use LLMs for grammar checking during the paper writing.

References

- Glenn W Brier. 1950. Verification of forecasts expressed in terms of probability. *Monthly weather review*, 78(1):1–3.
- Muthu Chidambaram and Rong Ge. 2024. Re-assessing how to compare and improve the calibration of machine learning models. *arXiv preprint arXiv:2406.04068*.
- Ke Fang, Tianyi Zhao, and Lu Cheng. 2025. Credence calibration game? calibrating large language models through structured play. *arXiv preprint arXiv:2508.14390*.

Jiahui Geng, Fengyu Cai, Yuxia Wang, Heinz Koepl, Preslav Nakov, and Iryna Gurevych. 2024. A survey of confidence estimation and calibration in large language models. In *Proceedings of the 2024 Conference of the North American Chapter of the Association for Computational Linguistics: Human Language Technologies (Volume 1: Long Papers)*, pages 6577–6595.

Aaron Grattafiori, Abhimanyu Dubey, Abhinav Jauhri, Abhinav Pandey, Abhishek Kadian, Ahmad Al-Dahle, Aiesha Letman, Akhil Mathur, Alan Schelten, Alex Vaughan, Amy Yang, Angela Fan, Anirudh Goyal, Anthony Hartshorn, Aobo Yang, Archi Mitra, Archie Sravankumar, Artem Korenev, Arthur Hinsvark, and 542 others. 2024. *The llama 3 herd of models*. *Preprint*, arXiv:2407.21783.

Chuan Guo, Geoff Pleiss, Yu Sun, and Kilian Q. Weinberger. 2017. *On calibration of modern neural networks*. In *Proceedings of the 34th International Conference on Machine Learning, ICML 2017, Sydney, NSW, Australia, 6-11 August 2017*, volume 70 of *Proceedings of Machine Learning Research*, pages 1321–1330. PMLR.

Daniel G Horvitz and Donovan J Thompson. 1952. A generalization of sampling without replacement from a finite universe. *Journal of the American Statistical Association*, 47(260):663–685.

Yue Huang, Lichao Sun, Haoran Wang, Siyuan Wu, Qihui Zhang, Yuan Li, Chujie Gao, Yixin Huang, Wenhan Lyu, Yixuan Zhang, and 1 others. 2024. Trustllm: Trustworthiness in large language models. *arXiv preprint arXiv:2401.05561*.

Mandar Joshi, Eunsol Choi, Daniel S Weld, and Luke Zettlemoyer. 2017. Triviaqa: A large scale distantly supervised challenge dataset for reading comprehension. In *Proceedings of the 55th Annual Meeting of the Association for Computational Linguistics (Volume 1: Long Papers)*, pages 1601–1611.

Saurav Kadavath, Tom Conerly, Amanda Askell, Tom Henighan, Dawn Drain, Ethan Perez, Nicholas Schiefer, Zac Hatfield-Dodds, Nova DasSarma, Eli Tran-Johnson, Scott Johnston, Sheer El-Showk, Andy Jones, Nelson Elhage, Tristan Hume, Anna Chen, Yuntao Bai, Sam Bowman, Stanislav Fort, and 17 others. 2022. *Language models (mostly) know what they know*. *Preprint*, arXiv:2207.05221.

Woosuk Kwon, Zhuohan Li, Siyuan Zhuang, Ying Sheng, Lianmin Zheng, Cody Hao Yu, Joseph E. Gonzalez, Hao Zhang, and Ion Stoica. 2023. *Efficient Memory Management for Large Language Model Serving with PagedAttention*. *Preprint*, arXiv:2309.06180.

Romain Lacombe, Kerrie Wu, and Eddie Dilworth. 2025. Don’t think twice! over-reasoning impairs confidence calibration. *arXiv preprint arXiv:2508.15050*.

- Balaji Lakshminarayanan, Alexander Pritzel, and Charles Blundell. 2017. [Simple and scalable predictive uncertainty estimation using deep ensembles](#). In *Advances in Neural Information Processing Systems 30: Annual Conference on Neural Information Processing Systems 2017, December 4-9, 2017, Long Beach, CA, USA*, pages 6402–6413.
- Potsawee Manakul, Adian Liusie, and Mark JF Gales. 2023. Selfcheckgpt: Zero-resource black-box hallucination detection for generative large language models. *arXiv preprint arXiv:2303.08896*.
- Zhiting Mei, Christina Zhang, Tenny Yin, Justin Lillard, Ola Shorinwa, and Anirudha Majumdar. 2025. Reasoning about uncertainty: Do reasoning models know when they don’t know? *arXiv preprint arXiv:2506.18183*.
- Matthias Minderer, Josip Djolonga, Rob Romijnders, Frances Hubis, Xiaohua Zhai, Neil Houlsby, Dustin Tran, and Mario Lucic. 2021. Revisiting the calibration of modern neural networks. *Advances in neural information processing systems*, 34:15682–15694.
- Peter Moskvichev and Dino Sejdinovic. 2025. All models are miscalibrated, but some less so: Comparing calibration with conditional mean operators. In *Australasian Joint Conference on Artificial Intelligence*, pages 274–287. Springer.
- Mahdi Pakdaman Naeni, Gregory F. Cooper, and Milos Hauskrecht. 2015. [Obtaining well calibrated probabilities using bayesian binning](#). In *Proceedings of the Twenty-Ninth AAAI Conference on Artificial Intelligence, January 25-30, 2015, Austin, Texas, USA*, pages 2901–2907. AAAI Press.
- Khanh Nguyen and Brendan O’Connor. 2015. Posterior calibration and exploratory analysis for natural language processing models. In *Proceedings of the 2015 Conference on Empirical Methods in Natural Language Processing*, pages 1587–1598.
- Alexandru Niculescu-Mizil and Rich Caruana. 2005. [Predicting good probabilities with supervised learning](#). In *Proceedings of the 22nd International Conference on Machine Learning*, pages 625–632. ACM.
- Jeremy Nixon, Michael W Dusenberry, Linchuan Zhang, Ghassen Jerfel, and Dustin Tran. 2019. Measuring calibration in deep learning. In *CVPR workshops*, volume 2.
- OpenAI, :, Sandhini Agarwal, Lama Ahmad, Jason Ai, Sam Altman, Andy Applebaum, Edwin Arbus, Rahul K. Arora, Yu Bai, Bowen Baker, Haiming Bao, Boaz Barak, Ally Bennett, Tyler Bertao, Nivedita Brett, Eugene Brevdo, Greg Brockman, Sebastian Bubeck, and 108 others. 2025. [gpt-oss-120b & gpt-oss-20b model card](#). *Preprint*, arXiv:2508.10925.
- Gabriel Pereyra, George Tucker, Jan Chorowski, Łukasz Kaiser, and Geoffrey Hinton. 2017. Regularizing neural networks by penalizing confident output distributions. *arXiv preprint arXiv:1701.06548*.
- John Platt and 1 others. 1999. Probabilistic outputs for support vector machines and comparisons to regularized likelihood methods. *Advances in large margin classifiers*, 10(3):61–74.
- Qwen, :, An Yang, Baosong Yang, Beichen Zhang, Binyuan Hui, Bo Zheng, Bowen Yu, Chengyuan Li, Dayiheng Liu, Fei Huang, Haoran Wei, Huan Lin, Jian Yang, Jianhong Tu, Jianwei Zhang, Jianxin Yang, Jiayi Yang, Jingren Zhou, and 25 others. 2025. [Qwen2.5 technical report](#). *Preprint*, arXiv:2412.15115.
- David Rein, Betty Li Hou, Asa Cooper Stickland, Jackson Petty, Richard Yuanzhe Pang, Julien Dirani, Julian Michael, and Samuel R. Bowman. 2023. [Gpqa: A graduate-level google-proof q&a benchmark](#). *Preprint*, arXiv:2311.12022.
- Paul R Rosenbaum and Donald B Rubin. 1983. The central role of the propensity score in observational studies for causal effects. *Biometrika*, 70(1):41–55.
- Chenglei Si, Chen Zhao, Sewon Min, and Jordan Boyd-Graber. 2022. Re-examining calibration: The case of question answering. In *Findings of the Association for Computational Linguistics: EMNLP 2022*, pages 2814–2829.
- Katherine Tian, Eric Mitchell, Allan Zhou, Archit Sharma, Rafael Rafailov, Huaxiu Yao, Chelsea Finn, and Christopher D Manning. 2023. Just ask for calibration: Strategies for eliciting calibrated confidence scores from language models fine-tuned with human feedback. In *Proceedings of the 2023 Conference on Empirical Methods in Natural Language Processing*, pages 5433–5442.
- Juozas Vaicenavicius, David Widmann, Carl Andersson, Fredrik Lindsten, Jacob Roll, and Thomas Schön. 2019. Evaluating model calibration in classification. In *The 22nd international conference on artificial intelligence and statistics*, pages 3459–3467. PMLR.
- Tu Vu, Mohit Iyyer, Xuezhi Wang, Noah Constant, Jerry Wei, Jason Wei, Chris Tar, Yun-Hsuan Sung, Denny Zhou, Quoc Le, and Thang Luong. 2023. [Freshllms: Refreshing large language models with search engine augmentation](#). *Preprint*, arXiv:2310.03214.
- Boxin Wang, Weixin Chen, Hengzhi Pei, Chulin Xie, Mintong Kang, Chenhui Zhang, Chejian Xu, Zidi Xiong, Ritik Dutta, Rylan Schaeffer, and 1 others. 2023. Decodingtrust: A comprehensive assessment of trustworthiness in {GPT} models.
- Xuezhi Wang, Jason Wei, Dale Schuurmans, Quoc Le, Ed Chi, Sharan Narang, Aakanksha Chowdhery, and Denny Zhou. 2022. Self-consistency improves chain of thought reasoning in language models. *arXiv preprint arXiv:2203.11171*.
- Yubo Wang, Xueguang Ma, Ge Zhang, Yuansheng Ni, Abhranil Chandra, Shiguang Guo, Weiming Ren, Aaran Arulraj, Xuan He, Ziyang Jiang, Tianle Li, Max Ku, Kai Wang, Alex Zhuang, Rongqi Fan, Xiang Yue,

- and Wenhui Chen. 2024. [Mmlu-pro: A more robust and challenging multi-task language understanding benchmark](#). *Preprint*, arXiv:2406.01574.
- Colin White, Samuel Dooley, Manley Roberts, Arka Pal, Ben Feuer, Siddhartha Jain, Ravid Shwartz-Ziv, Neel Jain, Khalid Saifullah, Sreemanti Dey, Shubh-Agrawal, Sandeep Singh Sandha, Siddhartha Naidu, Chinmay Hegde, Yann LeCun, Tom Goldstein, Willie Neiswanger, and Micah Goldblum. 2025. [Livebench: A challenging, contamination-limited llm benchmark](#). *Preprint*, arXiv:2406.19314.
- Miao Xiong, Zhiyuan Hu, Xinyang Lu, Yifei Li, Jie Fu, Junxian He, and Bryan Hooi. 2024. [Can llms express their uncertainty? an empirical evaluation of confidence elicitation in llms](#). In *The Twelfth International Conference on Learning Representations, ICLR 2024, Vienna, Austria, May 7-11, 2024*. OpenReview.net.
- An Yang, Anfeng Li, Baosong Yang, Beichen Zhang, Binyuan Hui, Bo Zheng, Bowen Yu, Chang Gao, Chengen Huang, Chenxu Lv, Chujie Zheng, Dayiheng Liu, Fan Zhou, Fei Huang, Feng Hu, Hao Ge, Haoran Wei, Huan Lin, Jialong Tang, and 41 others. 2025. [Qwen3 technical report](#). *Preprint*, arXiv:2505.09388.
- Dongkeun Yoon, Seungone Kim, Sohee Yang, Sunkyung Kim, Soyeon Kim, Yongil Kim, Eunbi Choi, Yireun Kim, and Minjoon Seo. 2025. Reasoning models better express their confidence. *arXiv preprint arXiv:2505.14489*.
- Bianca Zadrozny and Charles Elkan. 2002. Transforming classifier scores into accurate multiclass probability estimates. In *Proceedings of the eighth ACM SIGKDD international conference on Knowledge discovery and data mining*, pages 694–699.
- Qingcheng Zeng, Weihao Xuan, Leyang Cui, and Rob Voigt. 2025. Thinking out loud: Do reasoning models know when they’re right? In *Proceedings of the 2025 Conference on Empirical Methods in Natural Language Processing*, pages 1394–1407.

A General Analysis

A.1 Theoretical Analysis

Why accuracy is a confounder Global calibration metrics depend not only on how confidence is distributed, but also on the proportion of correct versus incorrect predictions. We formalize this mechanism in a deliberately controlled limit case, which is weaker than requiring uniform confidence across all predictions but is not intended as a full model of real LLM behavior.

Assumption 1 (Shared Conditional Confidence) *Two models M_A and M_B , evaluated on the same dataset, share identical conditional confidence distributions:*

- Correct ($z = 1$): confidence $c \sim P_1(c)$, with mean $\mu_1 = \mathbb{E}[c \mid z = 1]$ and variance $\sigma_1^2 = \text{Var}(c \mid z = 1)$.
- Incorrect ($z = 0$): confidence $c \sim P_0(c)$, with mean $\mu_0 = \mathbb{E}[c \mid z = 0]$ and variance $\sigma_0^2 = \text{Var}(c \mid z = 0)$.

The two models differ solely in their accuracy $a = \text{Acc}(M)$.

Under this assumption, the two models exhibit identical confidence *behavior* conditioned on correctness, differing only in how often they are right. This isolates accuracy as the only source of variation: any resulting calibration difference is attributable to accuracy rather than to intrinsic differences in uncertainty estimation. We use this as an illustrative sufficient case, not as a claim that real LLMs differ only in accuracy.

Proposition 1 (Limit-case: BS Linear in Accuracy)

Under Assumption 1, the Brier Score is a linear function of accuracy a . Let $L_0 = \sigma_0^2 + \mu_0^2$, $\Delta_L = \sigma_1^2 + (1 - \mu_1)^2 - \sigma_0^2 - \mu_0^2$. Then

$$\text{BS}(a) = L_0 + a \cdot \Delta_L.$$

Proof. By the law of total expectation, decompose the Brier Score by correctness:

$$\begin{aligned} \text{BS} &= \mathbb{E}[(c - z)^2] = a \cdot \mathbb{E}[(c - 1)^2 \mid z = 1] \\ &\quad + (1 - a) \cdot \mathbb{E}[c^2 \mid z = 0]. \end{aligned}$$

For the two conditional terms, applying the bias-

variance decomposition gives

$$\begin{aligned} \mathbb{E}[(c - 1)^2 \mid z = 1] &= \text{Var}(c \mid z = 1) \\ &\quad + (\mathbb{E}[c \mid z = 1] - 1)^2 \\ &= \sigma_1^2 + (1 - \mu_1)^2, \\ \mathbb{E}[c^2 \mid z = 0] &= \text{Var}(c \mid z = 0) \\ &\quad + (\mathbb{E}[c \mid z = 0])^2 = \sigma_0^2 + \mu_0^2. \end{aligned}$$

Substituting into Equation (1), we have

$$\begin{aligned} \text{BS}(a) &= a[\sigma_1^2 + (1 - \mu_1)^2] + (1 - a)[\sigma_0^2 + \mu_0^2] \\ &= [\sigma_0^2 + \mu_0^2] + a[\sigma_1^2 + (1 - \mu_1)^2 - \sigma_0^2 - \mu_0^2] \\ &= L_0 + a \cdot \Delta_L. \end{aligned}$$

□

Remark 1 (Slope condition is easily satisfied)

The condition $\Delta_L < 0$ holds when correct predictions deviate less from their ideal confidence than incorrect ones. Since the ideal confidence is 1 for correct predictions and 0 for incorrect ones, this reduces to

$$\sigma_1^2 + (1 - \mu_1)^2 < \sigma_0^2 + \mu_0^2,$$

which is readily satisfied in practice: well-functioning models assign higher confidence to correct predictions ($\mu_1 > \mu_0$), making $(1 - \mu_1)^2$ small, while overconfidence on incorrect predictions keeps μ_0^2 substantial. Consequently, higher accuracy mechanically improves BS even when the underlying confidence behavior is identical.

Remark 2 (Constant-confidence case) *When P_1 and P_0 both degenerate to a point mass at q , i.e., $\mu_1 = \mu_0 = q$ and $\sigma_1 = \sigma_0 = 0$, Proposition 1 simplifies to*

$$\text{BS}(a) = q^2 + a(1 - 2q),$$

recovering the toy example of Section 3.

A.2 Empirical Analysis

Extension to ECE. Unlike the Brier Score, ECE involves binning and absolute values, making a closed-form analysis less tractable. However, the key mechanism is analogous: as a increases, each confidence bin receives a higher proportion of correct predictions, pushing the bin-level accuracy $\text{acc}(S_b)$ closer to the bin-level confidence $\text{conf}(S_b)$ in the overconfident regime ($\text{acc}(S_b) \leq \text{conf}(S_b)$), thereby reducing the per-bin calibration gap and hence ECE.

Empirical Setup. We verify this empirically in Figure 1. Across five benchmarks spanning knowledge-based (TriviaQA, FreshQA) and reasoning-based tasks (MMLU-Pro, GPQA, LiveBench), we compare the ECE gap against the accuracy gap between stronger models and weaker models, covering both scale-based pairs (Qwen2.5 7B vs. 72B, LLaMA 3.1 8B vs. 70B, GPT-OSS 20B vs. 120B) and thinking vs. non-thinking pairs (Qwen3-8B and GPT-OSS under high/low reasoning settings). The results reveal a strong negative correlation ($\rho = -0.670$, $n = 40$, 95% CI $[-0.81, -0.45]$, $p < 10^{-5}$) between accuracy differences and raw ECE differences, consistent with our theoretical analysis: models with higher accuracy mechanically obtain better ECE scores even when their underlying confidence behavior is not correspondingly superior.

B Justification of Distribution-Aligned Calibration

Distribution-Aligned (DA) originates in survey sampling (Horvitz and Thompson, 1952) and is widely used in causal inference to correct for confounded comparisons between treatments and outcomes (Rosenbaum and Rubin, 1983). We briefly justify its application in our setting by making the analogy explicit.

Standard causal inference formulation. Consider a binary treatment $T \in \{0, 1\}$, an outcome Y , and a confounder X that influences both T and Y . The naïve comparison $\mathbb{E}[Y | T = 1] - \mathbb{E}[Y | T = 0]$ is biased whenever the distribution of X differs across treatment groups. DA removes this bias by reweighting each observation by the inverse of its treatment probability (propensity score), so that the weighted confounder distribution is balanced across groups.

Mapping to calibration comparison. In our setting, the role of the *treatment* T is played by model identity $m \in \{A, B\}$: comparing calibration across models is analogous to comparing outcomes across treatment arms. The *confounder* X corresponds to instance-level correctness $z_i^{(m)}$, which aggregates to model accuracy $a_m = \text{Acc}(M_m)$; just as a covariate that differs across treatment groups biases the naïve comparison, differing accuracy compositions confound the raw calibration comparison. The *outcome* Y maps to the per-instance calibration loss, e.g., $(c_i^{(m)} - z_i^{(m)})^2$ for

the Brier Score. The *propensity score* $P(T | X)$ corresponds to the probability of each correctness status in the source model, namely a_A for correct predictions ($z = 1$) and $1 - a_A$ for incorrect predictions ($z = 0$). Finally, the *target population* is the accuracy level of the reference model a_B , to which we wish to adjust the distribution of the results of the source model. Under this mapping, the weights

$$w_i^{(A)} = \begin{cases} a_B / a_A & \text{if } z_i^{(A)} = 1, \\ (1 - a_B) / (1 - a_A) & \text{if } z_i^{(A)} = 0, \end{cases}$$

are standard importance weights that transform the correctness distribution of M_A to match the target accuracy a_B . For each correctness class $z \in \{0, 1\}$, the weight equals the target proportion divided by the source proportion, which is precisely the density ratio form used in classical DA.

Assumptions. The validity of DA here requires two standard conditions: 1) *Positivity*: $0 < a_m < 1$, which holds trivially on any nontrivial benchmark; and 2) *Conditional exchangeability*: conditioned on correctness status z , the confidence distribution is comparable across the accuracy shift.

C Instruction Prompt Examples.

Answer Generation Prompts All models share the same answer-generation prompt family, with template selection determined by task type; reasoning behavior is controlled via model parameters rather than prompt wording. Specifically, we apply the multiple-choice template to GPQA Diamond and MMLU-Pro, the reasoning template to LiveBench, and the open-ended template to FreshQA and TriviaQA.

D Implementation Details

D.1 Model and Inference Details

We evaluate 14 locally deployed models spanning four families: Qwen2.5, LLaMA 3.1, Qwen3, and GPT-OSS. Table 10 lists all models. Qwen3 and GPT-OSS each expose a reasoning-intensity control: for Qwen3, the `enable_thinking` flag in the chat template switches between thinking (True) and non-thinking (False) modes; for GPT-OSS, the `reasoning_effort` parameter selects between high and low settings. This yields 14 model configurations in total. All models are served locally via vLLM (Kwon et al., 2023) in bfloat16 precision. Both answer-generation and confidence-estimation

I: MULTIPLE-CHOICE TEMPLATE
Task: Solve the following multiple-choice problem. The answer should be a single letter (A, B, C, D, etc.). Provide your final answer in the following format: <code>\boxed{A}</code> Problem: <code>{problem}</code>
II: REASONING TEMPLATE
Task: Solve the following reasoning problem. Provide your final answer in the following XML format: <code><answer>final answer here</answer></code> Problem: <code>{problem}</code>
III: OPEN-ENDED TEMPLATE
Task: Answer the following factual question directly. This is NOT a multiple-choice question. Provide a direct factual answer. Provide your final answer in the following XML format: <code><answer>final answer here</answer></code> Question: <code>{problem}</code>

Table 3: Three prompt templates used for generation across different task types.

stages share the same decoding configuration: temperature = 1.0, top- p = 1.0, and top- k = -1, with max_tokens set to max_model_len. Context lengths are 32,768 tokens for Qwen2.5 and Qwen3, 40,960 for LLaMA 3.1, and 131,072 for GPT-OSS.

D.2 Dataset Details and Evaluation Protocol

We evaluate on five datasets: FreshQA, TriviaQA, GPQA Diamond, LiveBench, and MMLU-Pro.

Dataset	Type	Size
FreshQA	Knowledge	600
TriviaQA	Knowledge	1,500
GPQA Diamond	Reasoning	198
LiveBench (reasoning subset)	Reasoning	200
MMLU-Pro	Reasoning	2,841

Table 4: Summary of the evaluation datasets used in our experiments.

FreshQA. We use the 2025-10-07 version of FreshQA and evaluate on 600 questions. This dataset is treated as an open-ended factual QA benchmark. Correctness is determined by LLM-based grading.

TriviaQA. We sample 1,500 examples from the unfiltered-nocontent validation split of TriviaQA. This dataset is treated as open-ended factual QA. We use alias-aware exact match, where a

prediction is counted as correct if it matches any acceptable alias.

GPQA Diamond. We use the standard GPQA Diamond split, containing 198 examples. This dataset is treated as an expert-level multiple-choice benchmark. Correctness is determined by exact matching between the extracted option letter and the gold answer.

LiveBench. We evaluate on 200 examples from the reasoning subset of LiveBench. This benchmark is treated as a reasoning / fill-in task. Correctness is determined by rule-based matching.

MMLU-Pro. We evaluate on 2,841 examples from the computer science, chemistry, and physics domains of MMLU-Pro. This dataset is treated as a multiple-choice benchmark. Correctness is determined by exact matching between the extracted option letter and the gold answer.

D.3 Confidence Elicitation Details

We consider three confidence estimation methods: verbalized confidence, $P(\text{True})$, and self-consistency.

Verbalized Confidence. The model is presented with the original question alongside its own full response and asked to assign a confidence score from 0 to 100. We use the full model_response rather than the extracted short answer as the answer source. We extract the numeric value inside `\boxed{}` and normalize it to $[0, 1]$ by dividing by 100.

VANILLA-VERB TEMPLATE
{Question}
Proposed Answer: {Answer}
How confident are you that the proposed answer is correct?
The confidence score should be a number from 0 (completely unsure) to 100 (absolutely certain).
Your response MUST strictly adhere to this format:
Confidence: <code>\boxed{Your confidence score from 0-100.}</code>
Now it is your turn to give a response:

Table 5: Vanilla verbalized confidence estimation template.

$P(\text{True})$. The model is presented with the original question alongside its own full response and asked to judge whether the proposed answer is true or false. Confidence is defined as the probability assigned to token A (“True”): we request

logprobs=20, extract the log-probability of token A, and convert it to a linear probability.

BINARY VERIFICATION TEMPLATE
{Question}
Proposed Answer: {Answer}
Is the proposed answer:
A. True
B. False
Output format: A or B only (single uppercase letter; no spaces, punctuation, or explanation):

Table 6: Binary verification template for answer correctness judgment.

Self-Consistency. For self-consistency, we generate 10 independent responses for each question using the same answer-generation prompt and decoding setup. The confidence of an example is defined as the fraction of runs whose extracted answer matches the extracted answer from the first run:

$$c_i = \frac{\sum_{k=1}^{10} \mathbf{1}[\hat{a}_k = \hat{a}_1]}{10}.$$

Here, \hat{a}_1 denotes the extracted answer from the first run and \hat{a}_k denotes the extracted answer from run k . If an example is marked as `is_attempted=False` in the first run, we skip it. If the answer is missing in later runs, the denominator remains 10.

E Additional Analyses

E.1 Reversal Rates on Knowledge and Reasoning Benchmarks

We further investigate whether ranking reversals are more prevalent on reasoning than knowledge benchmarks. Table 7 shows this pattern holds consistently under the DA and IA views, but varies under CA. Specifically, verbalized confidence yields higher reasoning reversal rates across all alignment views, whereas SC and $P(\text{true})$ diverge under CA. Additionally, Table 8 indicates that, aggregated across all methods and views, this reasoning-knowledge gap is driven primarily by mode/effort differences between evaluated models, rather than size differences.

Method	View	KRR	RRR	Δ (RRR-KRR)
SC	DA	6.2	41.7	+35.4
	IA	18.8	41.7	+22.9
	CA	56.2	41.7	-14.6
Verbalized	DA	43.8	58.3	+14.6
	IA	50.0	62.5	+12.5
	CA	18.8	33.3	+14.6
$P(\text{true})$	DA	37.5	54.2	+16.7
	IA	25.0	25.0	+0.0
	CA	50.0	20.8	-29.2

Table 7: Knowledge reversal rate (KRR) and reasoning reversal rate (RRR) broken down by confidence method and alignment view. For $\Delta(\text{RRR} - \text{KRR})$, positive values indicate reversal is more frequent on reasoning datasets.

Pair type	KRR	RRR	Δ (RRR-KRR)	#Pairs
mode/effort	33.3	45.2	+11.9	5
size	35.2	37.0	+1.9	3

Table 8: Average reversal gap by pair type after merging all confidence methods and aligned views. Positive Δ values indicate that reversal is more frequent on reasoning datasets.

E.2 Reversal Rates Across Accuracy-Gap Bins

We further examine how reversal rates change as the accuracy gap between the two compared models increases. Figure 5 shows that the pattern is better described as threshold-like than monotonic.

More concretely, when the accuracy gap is below 0.1, reversal rates are generally much lower across both the method-grouped and view-grouped panels. Once the gap exceeds 0.1, reversal becomes notice-

ably more common and remains at a substantially higher level. This indicates that reversal is much more likely once the two models are separated by a non-trivial gap in task accuracy.

At the same time, the figure does not support the stronger claim that reversal keeps increasing as the accuracy gap becomes larger and larger. After crossing the 0.1 threshold, the higher-gap bins fluctuate rather than rising monotonically. In other words, the key empirical dividing line is whether the accuracy gap is above 0.1, not which larger bin it falls into.

E.3 Both-Wrong and Both-Right Confidence Distributions

Figure 6 reveals several consistent patterns across methods and datasets. First, all three confidence methods show substantial separation between both-wrong and both-right examples: both-right mass is generally concentrated toward the high-confidence end, while both-wrong mass is shifted to the left. In this sense, all three methods preserve a meaningful distinction between clearly correct and clearly incorrect shared outcomes.

At the same time, the three methods differ in how sharply and how reliably they make this distinction. Verbalized confidence and $P(\text{true})$ are more polarized, with much of their mass pushed toward the two extremes. This produces visually sharp distributions, but it also reveals substantial overconfidence: both methods still assign considerable probability mass near the high-confidence end even on both-wrong examples. Among the three, verbalized confidence appears to show the weakest separation overall, with the red and blue mean lines often relatively close to each other, indicating that incorrect shared outcomes still receive fairly high confidence. $P(\text{true})$ shows a similar but somewhat less severe pattern.

SC behaves differently. Its distributions are broader and less concentrated at the extremes, so the distinction between both-wrong and both-right is less “all-or-nothing” but often more conservative. In particular, SC places less mass on extremely high confidence for both-wrong examples, making its overconfidence visibly weaker than that of verbalized confidence and $P(\text{true})$. This does not mean that SC is free of overconfidence—some datasets still show substantial overlap—but the figure suggests that its errors are less driven by extreme high-confidence mistakes.

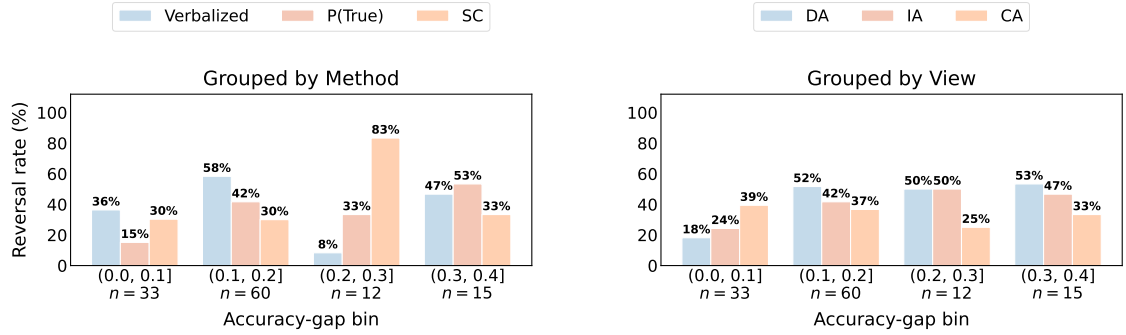


Figure 5: Reversal rate by accuracy-gap bin. The combined figure presents the same pattern from two complementary perspectives: grouped by confidence method and grouped by aligned view. In both views, reversal increases once the accuracy gap exceeds 0.1, but does not exhibit a clear monotonic increase across higher bins.

Both-Wrong vs Both-Right

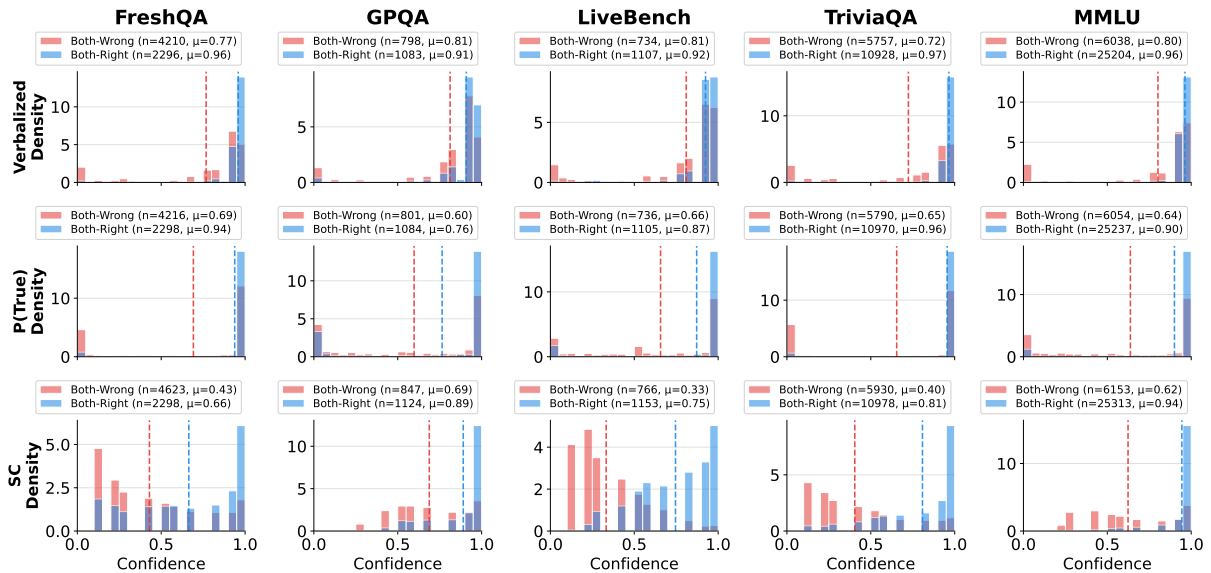


Figure 6: Histogram comparison of confidence distributions on both-wrong and both-right examples across three confidence elicitation methods and five datasets. The figure is intended as a descriptive view of how well the two shared-outcome regions are separated, and where overconfidence on both-wrong examples may appear.

E.4 Instance-Aligned Retention

Since IA compares models only on shared-outcome examples, one concern is that the retained subset might become too small to support stable conclusions. We therefore report the retained sample size for each model-pair-dataset cell. Retention is defined as $|D_{IA}|/|D|$, where $D_{IA} = D_{\text{both-right}} \cup D_{\text{both-wrong}}$. As shown in Table 9, IA retains substantial coverage across all 40 model-pair-dataset cells: the median retention is 78.0%, the IQR is [66.3%, 82.2%], and the minimum is 55.2%. No cell falls below 50%, indicating that the IA results are not driven by narrow retained subsets. Together with the aggregate correlation in Figure 1,

this suggests that the observed reversals reflect a systematic accuracy-related confound rather than sampling noise.

F Calibration Metrics

Tables 10–14 present the full calibration metrics underlying the trends visualized in Figures 2 and 3. For each of the five evaluation datasets (FreshQA, TriviaQA, GPQA Diamond, LiveBench Reasoning, and MMLU-Pro), we report accuracy and two calibration measures (*i.e.*, Brier Score and ECE), across three confidence elicitation methods (Verbalize, P(True), and Self-Consistency) and four evaluation views: **Raw**, **CA**, **DA** and **IA**. All accuracy

Pair	Type	FreshQA	GPQA	LiveBench	TriviaQA	MMLU-Pro
Qwen3-8B T/N	Mode	474 (79.0)	135 (68.2)	113 (56.5)	1181 (78.7)	2263 (79.7)
Qwen3-14B T/N	Mode	474 (79.0)	130 (65.7)	120 (60.0)	1229 (81.9)	2360 (83.1)
Qwen3-32B T/N	Mode	469 (78.2)	142 (71.7)	115 (57.5)	1208 (80.5)	2369 (83.4)
GPT-OSS-120B H/L	Effort	524 (87.3)	159 (80.3)	144 (72.0)	1356 (90.4)	2574 (90.6)
GPT-OSS-20B H/L	Effort	498 (83.0)	137 (69.2)	128 (64.0)	1215 (81.0)	2377 (83.7)
Qwen2.5 72B/7B	Size	446 (74.3)	123 (62.1)	133 (66.5)	1003 (66.9)	1797 (63.3)
LLaMA3.1 70B/8B	Size	331 (55.2)	124 (62.6)	154 (77.0)	1119 (74.6)	1706 (60.0)
GPT-OSS 120B/20B H	Size	480 (80.0)	168 (84.8)	179 (89.5)	1168 (77.9)	2654 (93.4)

Table 9: Instance-Aligned retained sample sizes across model-pair–dataset cells. Each cell reports $|D_{IA}|$ with the retention percentage in parentheses. Dataset sizes are 600 for FreshQA, 198 for GPQA Diamond, 200 for LiveBench Reasoning, 1,500 for TriviaQA, and 2,841 for MMLU-Pro. T/N denotes thinking versus non-thinking, and H/L denotes high versus low reasoning effort.

values are computed from a single run with temperature = 1. Each model pair is followed by a $\delta(\Delta)$ row showing the difference ($\text{Model}_1 - \text{Model}_2$), where **green** indicates the better-performing direction and **red** the worse.

Model	Acc	Raw		CA		DA		IA	
		Brier	ECE	Brier	ECE	Brier	ECE	Brier	ECE
<i>Verbalize</i>									
Qwen2.5-7B	21.4	53.3	53.3	49.5	45.9	52.2	56.8	49.6	54.6
Qwen2.5-72B	38.7	44.6	42.3	41.2	38.7	54.5	58.4	52.1	56.1
$\delta(\Delta)$	-17.3	+8.7	+11.0	+8.3	+7.2	-2.3	-1.6	-2.5	-1.5
Llama3.1-8B	32.1	48.5	50.7	44.9	44.2	45.1	47.2	43.7	46.6
Llama3.1-70B	49.3	32.1	32.9	32.6	31.6	50.5	51.9	49.0	50.5
$\delta(\Delta)$	-17.2	+16.3	+17.9	+12.3	+12.5	-5.4	-4.7	-5.3	-3.9
Qwen3-8B-nothink	26.8	57.0	60.7	53.8	56.7	57.1	61.0	57.6	61.7
Qwen3-8B-think	36.1	42.4	46.4	35.8	42.3	61.3	65.5	60.8	65.3
$\delta(\Delta)$	-9.3	+14.6	+14.3	+18.0	+14.4	-4.1	-4.5	-3.2	-3.6
Qwen3-32B-nothink	31.3	36.5	37.6	43.3	44.9	36.5	37.6	33.6	34.9
Qwen3-32B-think	41.6	50.7	52.8	45.0	47.6	59.5	62.4	57.4	60.5
$\delta(\Delta)$	-10.3	-14.2	-15.2	-1.7	-2.7	-23.0	-24.8	-23.8	-25.6
GPT-OSS-20B-low	35.8	39.5	42.0	31.2	32.4	39.5	42.0	39.3	43.1
GPT-OSS-20B-high	40.1	44.2	47.8	26.5	27.5	47.6	51.8	46.6	51.1
$\delta(\Delta)$	-4.3	-4.7	-5.7	+4.7	+4.9	-8.1	-9.7	-7.3	-8.0
GPT-OSS-120B-low	46.3	33.1	35.0	32.7	33.4	33.1	35.0	32.4	35.6
GPT-OSS-120B-high	47.8	33.6	37.2	32.8	34.4	34.5	38.4	33.8	38.3
$\delta(\Delta)$	-1.5	-0.5	-2.2	-0.1	-1.0	-1.4	-3.4	-1.4	-2.6
GPT-OSS-20B-high	40.1	44.2	47.8	26.5	27.5	47.6	51.8	46.6	51.1
GPT-OSS-120B-high	47.8	33.6	37.2	32.8	34.4	34.5	38.4	33.8	38.3
$\delta(\Delta)$	-7.7	+10.6	+10.5	-6.2	-6.9	+13.1	+13.3	+12.8	+12.9
<i>P(True)</i>									
Qwen2.5-7B	21.4	39.7	40.5	39.0	39.1	39.7	40.5	39.3	40.0
Qwen2.5-72B	38.7	31.4	31.6	26.0	25.6	38.7	41.4	36.8	39.8
$\delta(\Delta)$	-17.3	+8.3	+8.8	+13.0	+13.4	+1.0	-0.9	+2.6	+0.2
Llama3.1-8B	32.1	40.6	39.8	36.0	38.0	41.3	44.2	41.0	44.4
Llama3.1-70B	49.3	35.6	36.0	38.2	36.9	61.1	62.4	59.4	61.3
$\delta(\Delta)$	-17.2	+5.0	+3.7	-2.2	+1.1	-19.8	-18.1	-18.4	-17.0
Qwen3-8B-nothink	26.8	50.3	51.2	50.5	51.6	50.3	51.2	50.5	51.6
Qwen3-8B-think	36.1	66.5	66.7	65.5	65.8	66.5	66.7	65.5	65.8
$\delta(\Delta)$	-9.3	-16.2	-15.5	-14.9	-14.1	-16.2	-15.5	-14.9	-14.1
Qwen3-32B-nothink	31.3	33.6	36.5	40.8	42.1	33.6	36.5	32.7	36.0
Qwen3-32B-think	41.6	47.1	47.0	38.0	37.6	53.4	53.5	52.5	52.7
$\delta(\Delta)$	-10.3	-13.4	-10.5	+2.8	+4.5	-19.7	-17.0	-19.8	-16.7
GPT-OSS-20B-low	35.8	44.0	44.1	46.9	46.9	44.0	44.1	44.6	44.6
GPT-OSS-20B-high	40.1	51.7	51.7	46.5	46.6	55.4	55.5	54.8	54.8
$\delta(\Delta)$	-4.3	-7.6	-7.7	+0.4	+0.4	-11.4	-11.4	-10.2	-10.2
GPT-OSS-120B-low	46.3	39.6	39.6	43.0	43.1	39.6	39.6	39.1	39.1
GPT-OSS-120B-high	47.8	45.1	45.1	40.5	40.5	46.2	46.2	45.2	45.2
$\delta(\Delta)$	-1.5	-5.5	-5.5	+2.6	+2.6	-6.6	-6.6	-6.1	-6.1
GPT-OSS-20B-high	40.1	51.7	51.7	46.5	46.6	55.4	55.5	54.8	54.8
GPT-OSS-120B-high	47.8	45.1	45.1	40.5	40.5	46.2	46.2	45.2	45.2
$\delta(\Delta)$	-7.7	+6.6	+6.7	+6.0	+6.1	+9.2	+9.3	+9.5	+9.6
<i>Self-Consistency</i>									
Qwen2.5-7B	21.4	27.4	24.4	17.5	14.5	27.4	24.4	25.2	21.2
Qwen2.5-72B	38.7	33.5	29.9	24.5	14.7	38.0	38.2	36.1	36.5
$\delta(\Delta)$	-17.3	-6.1	-5.5	-7.0	-0.2	-10.6	-13.8	-10.9	-15.3
Llama3.1-8B	32.1	21.9	14.1	19.5	13.3	21.9	14.1	23.7	16.0
Llama3.1-70B	49.3	28.5	23.5	29.8	24.9	24.9	18.4	24.5	18.8
$\delta(\Delta)$	-17.2	-6.6	-9.4	-10.3	-11.6	-3.0	-4.2	-0.7	-2.8
Qwen3-8B-nothink	26.8	26.2	22.6	17.8	11.5	26.1	22.5	23.5	19.7
Qwen3-8B-think	36.1	23.0	15.0	23.1	16.2	20.8	14.3	19.8	14.1
$\delta(\Delta)$	-9.3	+3.3	+7.6	-5.3	-4.7	+5.3	+8.2	+3.8	+5.7
Qwen3-32B-nothink	31.3	24.7	18.4	20.2	14.0	24.7	18.4	24.5	17.5
Qwen3-32B-think	41.6	23.9	16.8	26.3	21.5	21.3	14.2	20.9	14.1
$\delta(\Delta)$	-10.3	+0.7	+1.6	-6.1	-7.5	+3.3	+4.3	+3.6	+3.4
GPT-OSS-20B-low	35.8	21.9	14.7	21.4	15.6	21.9	14.7	22.9	15.9
GPT-OSS-20B-high	40.1	25.6	18.3	26.2	19.9	23.6	16.7	23.7	17.8
$\delta(\Delta)$	-4.3	-3.7	-3.6	-4.8	-4.3	-1.8	-2.0	-0.8	-1.9
GPT-OSS-120B-low	46.3	29.4	23.7	28.3	22.7	29.4	23.7	30.6	25.1
GPT-OSS-120B-high	47.8	31.2	26.5	32.3	27.1	31.3	27.0	30.5	26.1
$\delta(\Delta)$	-1.5	-1.9	-2.8	-4.0	-4.4	-1.9	-3.3	+0.1	-1.1
GPT-OSS-20B-high	40.1	25.6	18.3	26.2	19.9	23.6	16.7	23.7	17.8
GPT-OSS-120B-high	47.8	31.2	26.5	32.3	27.1	31.3	27.0	30.5	26.1
$\delta(\Delta)$	-7.7	-5.7	-8.2	-6.0	-7.2	-7.7	-10.3	-6.8	-8.3

Table 10: Calibration metrics on **FreshQA**. For calibration metrics (Brier, ECE), lower is better (\downarrow). $\delta(\Delta)$ rows show the difference ($\text{Model}_1 - \text{Model}_2$). **Green**: better; **Red**: worse.

Model	Acc	Raw		CA		DA		IA	
		Brier	ECE	Brier	ECE	Brier	ECE	Brier	ECE
<i>Verbalize</i>									
Qwen2.5-7B	41.4	31.2	32.8	27.9	28.4	31.2	32.8	25.7	27.0
Qwen2.5-72B	71.7	20.5	20.6	18.3	18.6	38.7	40.0	26.7	27.6
$\delta(\Delta)$	-30.3	+10.7	+12.2	+9.6	+9.8	-7.5	-7.2	-1.0	-0.6
Llama3.1-8B	59.9	29.8	29.9	24.5	23.6	29.8	29.9	18.7	18.3
Llama3.1-70B	79.1	19.0	18.9	18.9	18.8	29.5	29.5	18.4	18.3
$\delta(\Delta)$	-19.2	+10.8	+11.0	+5.6	+4.8	+0.2	+0.4	+0.3	-0.1
Qwen3-8B-nothink	45.3	42.9	45.2	38.6	40.3	42.9	45.2	37.6	39.6
Qwen3-8B-think	60.3	32.4	33.8	30.1	32.5	44.5	47.4	37.5	40.2
$\delta(\Delta)$	-15.0	+10.5	+11.4	+8.5	+7.8	-1.5	-2.3	+0.2	-0.6
Qwen3-32B-nothink	54.1	24.7	25.1	27.2	27.7	24.7	25.1	21.3	21.7
Qwen3-32B-think	64.5	28.7	28.9	25.7	26.4	36.6	37.7	30.6	31.7
$\delta(\Delta)$	-10.4	-4.0	-3.8	+1.4	+1.3	-11.9	-12.6	-9.3	-10.0
GPT-OSS-20B-low	52.0	21.9	22.2	22.0	22.3	21.9	22.2	18.9	19.1
GPT-OSS-20B-high	60.3	24.3	25.0	25.3	25.7	29.1	31.1	24.6	27.0
$\delta(\Delta)$	-8.3	-2.4	-2.7	-3.3	-3.4	-7.2	-8.9	-5.6	-8.0
GPT-OSS-120B-low	74.9	12.0	10.8	12.4	11.0	12.0	10.8	10.4	8.6
GPT-OSS-120B-high	78.8	12.9	11.8	12.3	11.4	17.2	17.0	12.1	11.4
$\delta(\Delta)$	-3.9	-0.9	-0.9	+0.1	-0.4	-5.2	-6.2	-1.7	-2.8
GPT-OSS-20B-high	60.3	24.3	25.0	25.3	25.7	29.1	31.1	24.6	27.0
GPT-OSS-120B-high	78.8	12.9	11.8	12.3	11.4	17.2	17.0	12.1	11.4
$\delta(\Delta)$	-18.5	+11.4	+13.2	+13.0	+14.3	+11.9	+14.1	+12.5	+15.7
<i>P(True)</i>									
Qwen2.5-7B	41.4	25.9	25.9	26.0	25.7	25.9	25.9	22.7	22.6
Qwen2.5-72B	71.7	17.9	17.4	15.4	14.7	31.8	32.5	21.6	21.9
$\delta(\Delta)$	-30.3	+8.0	+8.4	+10.6	+11.0	-5.9	-6.6	+1.1	+0.7
Llama3.1-8B	59.9	26.0	25.0	21.9	19.1	26.0	25.0	17.3	14.4
Llama3.1-70B	79.1	17.1	15.6	17.2	15.9	29.5	29.8	18.2	17.9
$\delta(\Delta)$	-19.2	+9.0	+9.5	+4.8	+3.2	-3.4	-4.8	-0.9	-3.5
Qwen3-8B-nothink	45.3	38.2	38.6	34.8	34.9	38.2	38.6	35.1	35.3
Qwen3-8B-think	60.3	34.6	34.7	30.1	30.2	46.6	46.9	39.3	39.8
$\delta(\Delta)$	-15.0	+3.6	+3.9	+4.8	+4.8	-8.4	-8.4	-4.3	-4.5
Qwen3-32B-nothink	54.1	22.7	22.1	25.1	24.6	22.7	22.1	20.8	20.2
Qwen3-32B-think	64.5	29.6	29.5	24.2	24.0	35.8	35.8	30.1	30.1
$\delta(\Delta)$	-10.4	-6.9	-7.5	+0.9	+0.6	-13.1	-13.7	-9.3	-9.9
GPT-OSS-20B-low	52.0	25.0	25.1	26.8	26.8	25.0	25.1	22.3	22.3
GPT-OSS-20B-high	60.3	31.2	31.2	27.3	27.4	36.4	36.4	31.4	31.4
$\delta(\Delta)$	-8.3	-6.1	-6.2	-0.5	-0.5	-11.4	-11.4	-9.1	-9.1
GPT-OSS-120B-low	74.9	14.7	14.7	16.2	16.2	14.7	14.7	12.7	12.7
GPT-OSS-120B-high	78.8	19.1	19.1	16.9	16.9	24.8	24.8	18.1	18.1
$\delta(\Delta)$	-3.9	-4.3	-4.3	-0.6	-0.6	-10.1	-10.1	-5.4	-5.4
GPT-OSS-20B-high	60.3	31.2	31.2	27.3	27.4	36.4	36.4	31.4	31.4
GPT-OSS-120B-high	78.8	19.1	19.1	16.9	16.9	24.8	24.8	18.1	18.1
$\delta(\Delta)$	-18.5	+12.1	+12.1	+10.5	+10.5	+11.6	+11.7	+13.2	+13.2
<i>Self-Consistency</i>									
Qwen2.5-7B	41.4	17.9	8.9	13.6	7.8	17.9	8.9	18.1	12.2
Qwen2.5-72B	71.7	17.1	11.7	21.5	22.4	25.1	22.7	19.2	14.2
$\delta(\Delta)$	-30.3	+0.9	-2.7	-7.9	-14.6	-7.2	-13.8	-1.1	-2.1
Llama3.1-8B	59.9	23.8	19.4	23.3	21.6	23.8	19.4	26.8	28.0
Llama3.1-70B	79.1	18.8	17.0	25.2	30.0	18.7	11.8	17.0	13.9
$\delta(\Delta)$	-19.2	+5.0	+2.4	-1.9	-8.4	+5.1	+7.6	+9.7	+14.1
Qwen3-8B-nothink	45.3	19.8	11.9	14.8	4.9	19.8	11.9	17.4	9.0
Qwen3-8B-think	60.3	14.5	7.4	19.2	17.9	14.3	4.7	13.0	4.5
$\delta(\Delta)$	-15.0	+5.3	+4.4	-4.4	-13.0	+5.5	+7.2	+4.4	+4.5
Qwen3-32B-nothink	54.1	17.6	9.5	14.7	7.4	17.6	9.5	15.9	8.5
Qwen3-32B-think	64.5	14.7	11.3	18.2	18.2	13.8	7.3	13.3	8.2
$\delta(\Delta)$	-10.4	+2.9	-1.8	-3.5	-10.8	+3.8	+2.2	+2.6	+0.3
GPT-OSS-20B-low	52.0	17.4	13.3	17.6	15.9	17.4	13.3	18.0	14.7
GPT-OSS-20B-high	60.3	17.9	12.8	19.8	18.3	16.9	9.0	16.5	9.9
$\delta(\Delta)$	-8.3	-0.5	+0.4	-2.2	-2.4	+0.5	+4.2	+1.4	+4.8
GPT-OSS-120B-low	74.9	13.7	9.7	13.9	11.1	13.7	9.7	13.1	10.4
GPT-OSS-120B-high	78.8	14.6	10.8	15.7	13.1	15.1	9.9	14.1	10.2
$\delta(\Delta)$	-3.9	-0.9	-1.0	-1.8	-1.9	-1.4	-0.2	-0.9	+0.3
GPT-OSS-20B-high	60.3	17.9	12.8	19.8	18.3	16.9	9.0	16.5	9.9
GPT-OSS-120B-high	78.8	14.6	10.8	15.7	13.1	15.1	9.9	14.1	10.2
$\delta(\Delta)$	-18.5	+3.3	+2.1	+4.1	+5.2	+1.8	-0.9	+2.5	-0.2

Table 11: Calibration metrics on **TriviaQA**. For calibration metrics (Brier, ECE), lower is better (\downarrow). $\delta(\Delta)$ rows show the difference ($\text{Model}_1 - \text{Model}_2$). **Green**: better; **Red**: worse.

Model	Raw	Self		CA		DA		IA	
		Brier	ECE	Brier	ECE	Brier	ECE	Brier	ECE
<i>Verbalize</i>									
Qwen2.5-7B	33.3	52.5	54.8	48.6	49.3	54.7	57.1	50.1	52.1
Qwen2.5-72B	50.0	41.8	41.2	41.7	42.4	54.7	57.1	52.0	54.6
$\delta(\Delta)$	-16.7	+10.8	+13.6	+6.9	+6.9	0.0	0.0	-1.9	-2.5
Llama3.1-8B	18.7	61.9	63.7	54.6	54.9	61.9	63.7	62.9	64.8
Llama3.1-70B	39.9	43.6	45.5	39.7	40.8	47.0	50.4	53.3	56.6
$\delta(\Delta)$	-21.2	+18.3	+18.2	+14.9	+14.1	+14.9	+13.3	+9.5	+8.2
Qwen3-8B-nothink	46.0	41.9	42.5	32.5	29.5	45.5	45.5	38.0	36.7
Qwen3-8B-think	61.6	26.8	25.9	31.5	32.8	45.1	46.4	38.3	37.8
$\delta(\Delta)$	-15.6	+15.2	+16.6	+0.9	-3.3	+0.4	-0.9	-0.3	-1.1
Qwen3-32B-nothink	51.5	38.5	39.2	34.0	33.8	38.5	39.2	29.5	28.9
Qwen3-32B-think	67.7	31.9	31.9	35.9	35.8	45.4	46.2	35.8	36.0
$\delta(\Delta)$	-16.2	+6.6	+7.3	-1.9	-2.0	-6.9	-7.1	-6.3	-7.1
GPT-OSS-20B-low	56.6	24.2	19.7	25.8	20.0	24.2	19.7	12.8	7.6
GPT-OSS-20B-high	74.2	12.7	9.2	22.8	19.3	33.7	34.3	11.3	8.7
$\delta(\Delta)$	-17.6	+11.5	+10.5	+3.0	+0.7	-9.5	-14.6	+1.5	-1.1
GPT-OSS-120B-low	64.6	17.5	11.6	20.9	14.5	17.5	11.6	12.9	8.6
GPT-OSS-120B-high	81.3	14.5	11.2	15.5	12.9	26.3	26.1	15.6	14.2
$\delta(\Delta)$	-16.7	+2.9	+0.5	+5.4	+1.6	-8.8	-14.5	-2.7	-5.5
GPT-OSS-20B-high	74.2	12.7	9.2	22.8	19.3	33.7	34.3	11.3	8.7
GPT-OSS-120B-high	81.3	14.5	11.2	15.5	12.9	26.3	26.1	15.6	14.2
$\delta(\Delta)$	-7.1	-1.8	-2.0	+7.3	+6.4	+7.4	+8.2	-4.2	-5.5
<i>P(True)</i>									
Qwen2.5-7B	33.3	34.7	33.5	39.5	37.5	34.7	33.5	31.1	30.1
Qwen2.5-72B	50.0	40.3	39.1	34.8	32.0	47.4	48.2	46.4	48.8
$\delta(\Delta)$	-16.7	-5.6	-5.6	+4.8	+5.5	-12.7	-14.7	-15.3	-18.7
Llama3.1-8B	18.7	38.2	40.4	36.1	34.3	38.2	40.4	39.4	43.0
Llama3.1-70B	39.9	39.8	37.3	37.5	35.4	49.2	52.0	51.3	55.9
$\delta(\Delta)$	-21.2	-1.6	+3.1	-1.4	-1.2	-11.1	-11.6	-12.0	-12.9
Qwen3-8B-nothink	46.0	40.6	39.3	32.5	29.5	40.6	39.3	41.7	40.2
Qwen3-8B-think	61.6	26.8	25.9	31.5	32.8	47.5	47.9	43.4	43.6
$\delta(\Delta)$	-15.6	+13.8	+13.4	+0.9	-3.3	-6.9	-8.6	-1.7	-3.4
Qwen3-32B-nothink	51.5	32.1	28.8	32.0	28.9	32.1	28.8	28.8	25.2
Qwen3-32B-think	67.7	38.1	38.1	38.2	38.1	47.8	47.7	41.4	41.4
$\delta(\Delta)$	-16.2	-6.0	-9.3	-6.2	-9.2	-15.7	-18.9	-12.6	-16.2
GPT-OSS-20B-low	56.6	29.9	30.2	36.8	37.0	29.9	30.2	23.9	24.2
GPT-OSS-20B-high	74.2	17.4	17.6	22.5	22.7	38.7	38.8	17.4	17.4
$\delta(\Delta)$	-17.6	+12.5	+12.7	+14.4	+14.3	-8.8	-8.6	+6.5	+6.8
GPT-OSS-120B-low	64.6	28.5	28.5	27.2	27.0	28.5	28.5	19.4	19.4
GPT-OSS-120B-high	81.3	25.2	25.2	25.0	25.0	39.5	39.5	25.2	25.2
$\delta(\Delta)$	-16.7	+3.2	+3.3	+2.2	+1.9	-11.0	-10.9	-5.7	-5.8
GPT-OSS-20B-high	74.2	17.4	17.6	22.5	22.7	38.7	38.8	17.4	17.4
GPT-OSS-120B-high	81.3	25.2	25.2	25.0	25.0	39.5	39.5	25.2	25.2
$\delta(\Delta)$	-7.1	-7.8	-7.7	-2.5	-2.3	-0.7	-0.7	-7.7	-7.7
<i>Self-Consistency</i>									
Qwen2.5-7B	33.3	55.5	56.2	32.5	34.7	55.5	56.2	52.5	54.1
Qwen2.5-72B	50.0	32.4	34.1	32.5	34.7	32.4	34.1	32.5	34.7
$\delta(\Delta)$	-16.7	+23.2	+22.1	0.0	0.0	+23.2	+22.1	+19.9	+19.3
Llama3.1-8B	18.7	18.9	17.5	17.2	20.2	18.9	17.5	17.2	20.2
Llama3.1-70B	39.9	28.3	32.5	28.7	34.0	28.3	32.5	28.7	34.0
$\delta(\Delta)$	-21.2	-9.4	-14.9	-11.5	-13.9	-9.4	-14.9	-11.5	-13.9
Qwen3-8B-nothink	46.0	23.2	12.8	20.1	13.5	23.2	14.6	24.1	15.4
Qwen3-8B-think	61.6	23.2	18.0	22.0	12.7	29.4	27.5	26.4	24.4
$\delta(\Delta)$	-15.6	0.0	-5.2	-1.9	+0.8	-6.2	-12.9	-2.3	-9.0
Qwen3-32B-nothink	51.5	20.3	13.7	15.2	10.5	20.3	13.7	17.8	10.6
Qwen3-32B-think	67.7	18.8	14.8	17.8	9.2	26.1	26.0	20.5	20.5
$\delta(\Delta)$	-16.2	+1.5	-1.1	-2.6	+1.3	-5.8	-12.3	-2.8	-9.9
GPT-OSS-20B-low	56.6	18.4	14.8	12.2	10.4	18.4	14.8	16.9	13.5
GPT-OSS-20B-high	74.2	15.7	13.0	15.8	6.9	22.1	22.5	16.8	18.4
$\delta(\Delta)$	-17.6	+2.7	+1.8	-3.6	+3.5	-3.7	-7.7	+0.1	-4.9
GPT-OSS-120B-low	64.6	19.5	15.2	13.0	10.0	19.5	15.2	14.3	10.9
GPT-OSS-120B-high	81.3	11.0	9.9	12.3	7.2	15.4	16.0	11.0	10.1
$\delta(\Delta)$	-16.7	+8.5	+5.2	+0.6	+2.8	+4.0	-0.9	+3.3	+0.8
GPT-OSS-20B-high	74.2	15.7	13.0	15.8	6.9	22.1	22.5	16.8	18.4
GPT-OSS-120B-high	81.3	11.0	9.9	12.3	7.2	15.4	16.0	11.0	10.1
$\delta(\Delta)$	-7.1	+4.6	+3.1	+3.5	-0.3	+6.7	+6.5	+5.8	+8.2

Table 12: Calibration metrics on **GPQA Diamond**. For calibration metrics (Brier, ECE), lower is better (\downarrow). $\delta(\Delta)$ rows show the difference ($\text{Model}_1 - \text{Model}_2$). **Green**: better; **Red**: worse.

Model	Acc	Raw		CA		DA		IA	
		Brier	ECE	Brier	ECE	Brier	ECE	Brier	ECE
<i>Verbalize</i>									
Qwen2.5-7B	17.0	70.6	74.1	64.5	67.0	73.0	76.8	71.2	75.7
Qwen2.5-72B	36.5	55.9	57.9	60.5	64.8	73.0	76.8	74.2	78.4
$\delta(\Delta)$	-19.5	+14.7	+16.2	+4.0	+2.3	0.0	0.0	-3.1	-2.7
Llama3.1-8B	9.5	70.5	73.0	65.1	66.8	70.5	73.0	70.7	73.9
Llama3.1-70B	22.5	52.1	53.8	44.7	47.8	57.1	60.3	59.0	62.5
$\delta(\Delta)$	-13.0	+18.4	+19.2	+20.4	+19.0	+13.4	+12.7	+11.7	+11.5
Qwen3-8B-nothink	38.5	55.6	55.4	21.3	19.1	53.5	55.1	31.5	30.8
Qwen3-8B-think	77.0	17.3	16.0	37.6	38.5	49.4	53.4	29.0	30.7
$\delta(\Delta)$	-38.5	+38.3	+39.4	-16.3	-19.4	+4.1	+1.8	+2.4	+0.0
Qwen3-32B-nothink	47.0	43.7	44.5	27.7	27.8	43.7	44.5	18.9	17.3
Qwen3-32B-think	85.5	12.0	11.7	27.4	27.8	40.7	43.1	17.3	18.1
$\delta(\Delta)$	-38.5	+31.7	+32.8	+0.3	0.0	+3.0	+1.4	+1.6	-0.7
GPT-OSS-20B-low	59.5	16.5	8.9	23.8	20.8	16.5	8.9	8.5	16.3
GPT-OSS-20B-high	89.5	2.2	6.3	16.9	14.9	13.7	14.8	2.2	7.4
$\delta(\Delta)$	-30.0	+14.3	+2.6	+7.0	+5.9	+2.8	-5.9	+6.3	+8.8
GPT-OSS-120B-low	69.0	9.1	6.5	23.8	20.8	9.1	6.5	6.0	13.2
GPT-OSS-120B-high	93.0	3.0	6.4	8.5	5.2	9.4	11.0	2.5	5.2
$\delta(\Delta)$	-24.0	+6.1	+0.1	+15.4	+15.5	-0.3	-4.6	+3.4	+8.0
GPT-OSS-20B-high	89.5	2.2	6.3	16.9	14.9	13.7	14.8	2.2	7.4
GPT-OSS-120B-high	93.0	3.0	6.4	8.5	5.2	9.4	11.0	2.5	5.2
$\delta(\Delta)$	-3.5	-0.8	-0.1	+8.4	+9.7	+4.3	+3.7	-0.3	+2.2
<i>P(True)</i>									
Qwen2.5-7B	17.0	59.1	61.4	57.6	59.2	59.1	61.4	57.2	59.6
Qwen2.5-72B	36.5	54.1	54.3	52.7	54.6	69.8	71.6	72.3	73.5
$\delta(\Delta)$	-19.5	+5.0	+7.1	+5.0	+4.6	-10.7	-10.2	-15.1	-13.9
Llama3.1-8B	9.5	34.9	45.9	38.8	46.9	34.9	45.9	34.4	47.8
Llama3.1-70B	22.5	52.1	53.8	44.7	47.8	62.2	69.9	64.7	73.3
$\delta(\Delta)$	-13.0	-17.2	-7.9	-5.9	-0.9	-27.3	-24.1	-30.3	-25.6
Qwen3-8B-nothink	38.5	45.1	45.5	34.0	33.3	45.1	45.5	34.0	33.3
Qwen3-8B-think	77.0	29.0	30.0	29.0	30.0	46.9	49.5	29.0	30.0
$\delta(\Delta)$	-38.5	+16.1	+15.5	+5.0	+3.3	-1.9	-4.1	+5.0	+3.3
Qwen3-32B-nothink	47.0	30.3	28.0	19.5	17.4	30.3	28.0	22.5	24.6
Qwen3-32B-think	85.5	12.8	13.0	21.3	21.0	40.0	40.6	18.7	19.0
$\delta(\Delta)$	-38.5	+17.4	+15.0	-1.8	-3.7	-9.7	-12.6	+3.8	+5.6
GPT-OSS-20B-low	59.5	21.9	22.2	15.3	15.7	21.9	22.2	12.7	12.8
GPT-OSS-20B-high	89.5	6.2	6.2	12.7	13.0	23.3	23.3	3.9	3.9
$\delta(\Delta)$	-30.0	+15.7	+16.0	+2.6	+2.8	-1.4	-1.1	+8.8	+8.9
GPT-OSS-120B-low	69.0	15.0	15.0	9.4	9.3	15.0	15.0	12.5	12.5
GPT-OSS-120B-high	93.0	4.5	4.5	5.0	5.0	16.2	16.2	3.5	3.5
$\delta(\Delta)$	-24.0	+10.5	+10.5	+4.4	+4.3	-1.2	-1.3	+9.0	+9.0
GPT-OSS-20B-high	89.5	6.2	6.2	12.7	13.0	23.3	23.3	3.9	3.9
GPT-OSS-120B-high	93.0	4.5	4.5	5.0	5.0	16.2	16.2	3.5	3.5
$\delta(\Delta)$	-3.5	+1.8	+1.7	+7.7	+8.0	+7.1	+7.0	+0.4	+0.4
<i>Self-Consistency</i>									
Qwen2.5-7B	17.0	20.0	18.8	12.3	16.0	20.0	18.8	19.5	20.2
Qwen2.5-72B	36.5	14.5	11.8	12.3	16.0	14.5	11.8	12.3	16.0
$\delta(\Delta)$	-19.5	+5.5	+7.0	0.0	0.0	+5.5	+7.0	+7.2	+4.2
Llama3.1-8B	9.5	7.8	5.3	6.5	7.0	7.8	5.3	6.5	7.0
Llama3.1-70B	22.5	8.5	8.8	7.2	11.9	8.5	8.8	7.2	11.9
$\delta(\Delta)$	-13.0	-0.7	-3.5	-0.8	-4.9	-0.7	-3.5	-0.8	-4.9
Qwen3-8B-nothink	38.5	17.0	7.6	11.8	10.1	17.0	8.6	21.9	21.9
Qwen3-8B-think	77.0	12.5	15.3	22.4	33.7	9.8	9.0	9.2	8.8
$\delta(\Delta)$	-38.5	+4.5	-7.8	-10.6	-23.6	+7.2	-0.4	+12.7	+13.1
Qwen3-32B-nothink	47.0	16.4	8.8	9.1	10.1	16.4	8.8	20.9	27.0
Qwen3-32B-think	85.5	11.8	17.4	22.0	33.5	10.0	8.0	9.4	9.3
$\delta(\Delta)$	-38.5	+4.6	-8.7	-12.8	-23.4	+6.4	+0.8	+11.5	+17.7
GPT-OSS-20B-low	59.5	16.1	18.1	13.2	19.0	16.3	18.7	26.6	43.6
GPT-OSS-20B-high	89.5	16.9	27.2	26.6	43.7	12.3	9.3	10.7	19.2
$\delta(\Delta)$	-30.0	-0.7	-9.0	-13.3	-24.6	+4.0	+9.4	+15.8	+24.3
GPT-OSS-120B-low	69.0	19.2	17.4	16.9	20.1	19.6	18.9	24.2	35.7
GPT-OSS-120B-high	93.0	10.6	18.6	18.4	31.7	8.4	8.7	10.4	17.3
$\delta(\Delta)$	-24.0	+8.5	-1.3	-1.5	-11.6	+11.1	+10.2	+13.8	+18.4
GPT-OSS-20B-high	89.5	16.9	27.2	26.6	43.7	12.3	9.3	10.7	19.2
GPT-OSS-120B-high	93.0	10.6	18.6	18.4	31.7	8.4	8.7	10.4	17.3
$\delta(\Delta)$	-3.5	+6.2	+8.5	+8.2	+12.0	+3.9	+0.7	+0.3	+1.9

Table 13: Calibration metrics on **LiveBench**. For calibration metrics (Brier, ECE), lower is better (\downarrow). $\delta(\Delta)$ rows show the difference ($\text{Model}_1 - \text{Model}_2$). **Green**: better; **Red**: worse.

Model	Acc	Raw		CA		DA		IA	
		Brier	ECE	Brier	ECE	Brier	ECE	Brier	ECE
<i>Verbalize</i>									
Qwen2.5-7B	49.0	43.6	44.8	33.9	34.2	43.6	44.8	28.4	28.3
Qwen2.5-72B	71.6	23.9	23.0	30.9	31.1	42.1	43.6	27.7	28.0
$\delta(\Delta)$	-22.6	+19.7	+21.8	+3.1	+3.0	+1.5	+1.2	+0.8	+0.3
Llama3.1-8B	31.6	56.7	57.3	47.3	47.5	57.0	57.7	48.8	49.4
Llama3.1-70B	57.6	28.3	28.5	28.3	28.5	39.5	40.2	33.3	34.1
$\delta(\Delta)$	-26.0	+28.4	+28.8	+19.0	+19.0	+17.5	+17.4	+15.6	+15.3
Qwen3-8B-nothink	70.9	25.2	25.1	19.2	19.1	25.2	25.1	12.6	11.4
Qwen3-8B-think	85.6	13.1	12.6	16.5	16.3	25.9	26.1	13.0	12.7
$\delta(\Delta)$	-14.7	+12.1	+12.5	+2.7	+2.8	-0.6	-0.9	-0.5	-1.3
Qwen3-32B-nothink	76.6	18.7	18.1	14.4	13.7	18.7	18.1	9.6	8.0
Qwen3-32B-think	88.6	11.2	10.5	15.2	14.4	21.2	21.0	10.6	10.0
$\delta(\Delta)$	-12.0	+7.5	+7.6	-0.8	-0.7	-2.5	-2.9	-1.0	-2.0
GPT-OSS-20B-low	74.8	15.9	12.1	12.8	9.1	16.0	12.2	9.1	4.9
GPT-OSS-20B-high	86.7	10.5	7.9	12.4	9.7	20.3	19.0	10.1	7.7
$\delta(\Delta)$	-11.9	+5.3	+4.2	+0.4	-0.6	-4.3	-6.9	-1.0	-2.9
GPT-OSS-120B-low	85.2	10.6	6.6	10.0	6.7	10.6	6.6	7.3	3.2
GPT-OSS-120B-high	88.2	8.9	6.3	9.1	6.1	11.2	9.0	7.4	5.0
$\delta(\Delta)$	-3.0	+1.7	+0.3	+0.9	+0.7	-0.6	-2.4	-0.1	-1.8
GPT-OSS-20B-high	86.7	10.5	7.9	12.4	9.7	20.3	19.0	10.1	7.7
GPT-OSS-120B-high	88.2	8.9	6.3	9.1	6.1	11.2	9.0	7.4	5.0
$\delta(\Delta)$	-1.5	+1.7	+1.6	+3.3	+3.7	+9.1	+10.1	+2.7	+2.8
<i>P(True)</i>									
Qwen2.5-7B	49.0	33.7	32.7	29.4	28.3	33.7	32.7	26.1	25.3
Qwen2.5-72B	71.6	20.6	19.2	21.1	19.5	31.4	30.6	20.9	20.0
$\delta(\Delta)$	-22.6	+13.0	+13.5	+8.3	+8.8	+2.2	+2.1	+5.2	+5.3
Llama3.1-8B	31.6	28.6	25.6	28.9	19.9	28.6	25.6	25.8	18.9
Llama3.1-70B	57.6	27.5	26.0	28.3	28.1	40.6	43.2	34.6	37.0
$\delta(\Delta)$	-26.0	+1.1	-0.4	+0.6	-8.2	-11.9	-17.6	-8.9	-18.2
Qwen3-8B-nothink	70.9	23.4	21.3	20.3	19.2	23.4	21.3	16.2	15.2
Qwen3-8B-think	85.6	19.7	19.6	20.3	19.8	30.3	29.2	19.5	19.4
$\delta(\Delta)$	-14.7	+3.7	+1.7	+0.0	-0.6	-6.9	-7.8	-3.3	-4.2
Qwen3-32B-nothink	76.6	14.9	11.3	13.0	10.7	14.9	11.3	12.2	11.6
Qwen3-32B-think	88.6	13.0	13.1	15.3	15.2	22.9	22.8	12.7	12.7
$\delta(\Delta)$	-12.0	+1.9	-1.7	-2.3	-4.5	-8.0	-11.5	-0.5	-1.1
GPT-OSS-20B-low	74.8	20.1	19.9	30.1	30.0	20.1	19.9	13.6	13.6
GPT-OSS-20B-high	86.7	16.1	16.2	14.7	14.7	25.3	25.3	15.6	15.7
$\delta(\Delta)$	-11.9	+4.0	+3.7	+15.4	+15.2	-5.2	-5.4	-2.1	-2.1
GPT-OSS-120B-low	85.2	14.5	14.6	15.4	15.3	14.5	14.6	10.0	10.0
GPT-OSS-120B-high	88.2	21.7	21.8	17.2	17.3	23.4	23.5	20.2	20.2
$\delta(\Delta)$	-3.0	-7.2	-7.2	-1.8	-2.0	-8.9	-8.9	-10.2	-10.2
GPT-OSS-20B-high	86.7	16.1	16.2	14.7	14.7	25.3	25.3	15.6	15.7
GPT-OSS-120B-high	88.2	21.7	21.8	17.2	17.3	23.4	23.5	20.2	20.2
$\delta(\Delta)$	-1.5	-5.6	-5.6	-2.5	-2.5	+1.9	+1.8	-4.5	-4.5
<i>Self-Consistency</i>									
Qwen2.5-7B	49.0	19.5	13.6	11.0	8.9	19.5	13.6	16.2	6.1
Qwen2.5-72B	71.6	12.8	6.3	14.6	9.7	19.3	19.4	13.6	13.4
$\delta(\Delta)$	-22.6	+6.7	+7.3	-3.6	-0.8	+0.2	-5.9	+2.6	-7.2
Llama3.1-8B	31.6	16.1	6.8	9.9	7.4	16.1	6.7	14.9	5.7
Llama3.1-70B	57.6	13.1	5.0	16.5	13.1	14.9	15.8	12.5	14.5
$\delta(\Delta)$	-26.0	+3.0	+1.8	-6.6	-5.7	+1.2	-9.1	+2.4	-8.8
Qwen3-8B-nothink	70.9	11.5	4.8	7.8	4.5	11.5	4.8	9.1	5.3
Qwen3-8B-think	85.6	9.2	6.9	9.7	5.7	17.0	16.9	8.9	8.9
$\delta(\Delta)$	-14.7	+2.3	-2.0	-1.9	-1.2	-5.5	-12.1	+0.2	-3.6
Qwen3-32B-nothink	76.6	9.0	4.1	6.3	3.5	9.0	4.1	7.6	4.9
Qwen3-32B-think	88.6	7.1	5.0	7.7	4.6	13.3	12.9	6.9	6.3
$\delta(\Delta)$	-12.0	+1.9	-0.9	-1.5	-1.1	-4.3	-8.8	+0.8	-1.4
GPT-OSS-20B-low	74.8	10.1	4.6	7.2	4.4	10.1	4.6	8.8	5.5
GPT-OSS-20B-high	86.7	8.3	6.5	8.6	4.7	14.7	14.6	8.3	8.0
$\delta(\Delta)$	-11.9	+1.8	-1.9	-1.4	-0.2	-4.6	-10.0	+0.5	-2.5
GPT-OSS-120B-low	85.2	9.0	6.3	7.2	5.1	9.0	6.3	7.3	5.2
GPT-OSS-120B-high	88.2	7.5	6.5	7.6	5.0	9.2	8.6	6.6	6.5
$\delta(\Delta)$	-3.0	+1.6	-0.2	-0.4	+0.0	-0.2	-2.2	+0.8	-1.2
GPT-OSS-20B-high	86.7	8.3	6.5	8.6	4.7	14.7	14.6	8.3	8.0
GPT-OSS-120B-high	88.2	7.5	6.5	7.6	5.0	9.2	8.6	6.6	6.5
$\delta(\Delta)$	-1.5	+0.8	0.0	+1.0	-0.4	+5.4	+6.1	+1.7	+1.6

Table 14: Calibration metrics on **MMLU-Pro**. For calibration metrics (Brier, ECE), lower is better (\downarrow). $\delta(\Delta)$ rows show the difference ($\text{Model}_1 - \text{Model}_2$). **Green**: better; **Red**: worse.